Journal of Medicinal Chemistry

pubs.acs.org/jmc

Article

Discovery and Optimization of Novel Pyrazolopyrimidines as Potent and Orally Bioavailable Allosteric HIV-1 Integrase Inhibitors

Guo Li,* Nicholas A. Meanwell, Mark R. Krystal, David R. Langley, B. Narasimhulu Naidu, Prasanna Sivaprakasam, Hal Lewis, Kevin Kish, Javed A. Khan, Alicia Ng, George L. Trainor, Christopher Cianci, Ira B. Dicker, Michael A. Walker, Zeyu Lin, Tricia Protack, Linda Discotto, Susan Jenkins, Samuel W. Gerritz, and Annapurna Pendri*

Cite This: https://dx.doi.org/10.1021/acs.jmedchem.9b01681

Read Online

ACCESS | Metrics & More | Article Recommendations | Supporting Information

ABSTRACT: The standard of care for HIV-1 infection, highly active antiretroviral therapy (HAART), combines two or more drugs from at least two classes. Even with the success of HAART, new drugs with novel mechanisms are needed to combat viral resistance, improve adherence, and mitigate toxicities. Active site inhibitors of HIV-1 integrase are clinically validated for the treatment of HIV-1 infection. Here we describe allosteric inhibitors of HIV-1 integrase that bind to the LEDGF/p75 interaction site and disrupt the structure of the integrase multimer that is required for the HIV-1 maturation. A series of pyrazolopyrimidine-based inhibitors was developed with a vector in the 2-position that was optimized by structure-guided compound design. This resulted in the discovery of pyrazolopyrimidine **3**, which was optimized at the 2- and 7-positions to afford **26** and **29** as potent allosteric inhibitors of HIV-1 integrase that exhibited low nanomolar antiviral potency in cell culture and encouraging PK properties.

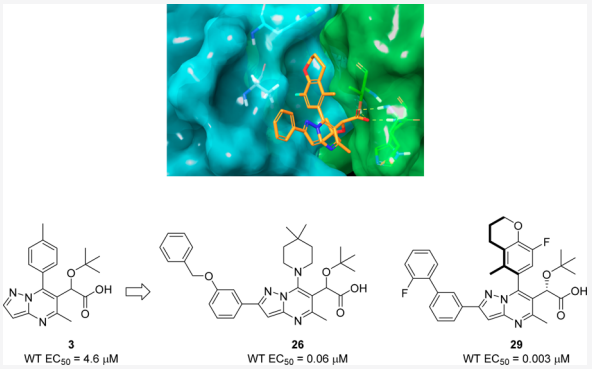

INTRODUCTION

Human immunodeficiency virus type 1 (HIV-1) is the etiologic agent underlying acquired immunodeficiency syndrome (AIDS) and was first recognized and diagnosed in the early 1980s. After more than 30 years, HIV-1 infection remains a significant medical problem and is now a global epidemic that infects 37 million people worldwide. At present, more than 40 drugs have been approved for the treatment of HIV-1/AIDS and these are used to create combination regimens designed to mitigate the emergence of resistance. These drugs belong mainly to four classes: nucleoside and non-nucleoside inhibitors of reverse transcriptase, integrase (IN) inhibitors, and inhibitors of HIV-1 protease.[1] In addition, the HIV-1 entry inhibitors maraviroc (a CCR5 co-receptor antagonist), enfuvirtide (a peptidic inhibitor of gp41 fusion), and ibalizumab (a nonimmunosuppressive monoclonal antibody that binds to the host cell receptor CD4) are available for later lines of therapy. Key challenges have been the continued emergence of resistance and the long-term toxicity associated with approved anti-HIV-1 drugs. The identification of additional viral targets and the development of new classes of antiviral compounds are essential in the continued fight against HIV/AIDS.

HIV-1 integrase is the enzyme responsible for integrating viral DNA into the host cell genome. Active site-targeted integrase strand transfer inhibitors (INSTIs) are clinically useful therapeutics that include raltegravir, elvitegravir, dolutegravir, and bictegravir (Figure 1).[2] These inhibitors bind to the active site of the integrase enzyme, forming a ternary complex with 3′ processed proviral DNA that impairs strand transfer activity, the step that initiates the integration of viral DNA into host DNA. In contrast, the allosteric integrase inhibitors (ALLINIs) bind to a site located at the HIV-1 integrase dimer interface that is recognized by the host cell transcription factor lens epithelium-derived growth factor (LEDGF/p75).[3−5] The important role of LEDGF/p75 in HIV-1 integration has been validated in vitro by site-directed mutagenesis studies,[6,7] RNAi knockdown experiments, and cellular expression of the integrase binding domain (IBD) of LEDGF that inhibits HIV-1 replication in cell culture.[8,9] Recent studies showed that the multifunctional ALLINIs not only inhibit IN binding to its cofactor LEDGF/p75 but also promote aberrant IN multimerization to block viral maturation, leading to the production of structurally defective,

Special Issue: Women in Medicinal Chemistry

Received: October 10, 2019

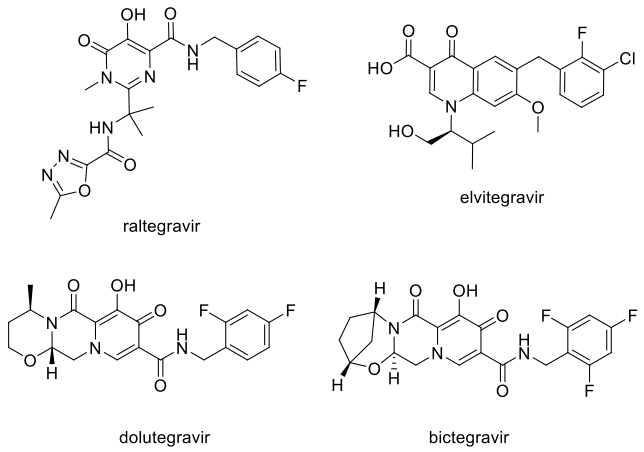

Figure 1. Structures of Food and Drug Administration (FDA)-approved HIV-1 active site-targeted integrase strand transfer inhibitors.

noninfectious virions.[10−13] The pleiotropic effects of ALLINIs suggest considerable promise as antiviral agents for the development of HIV-1 therapeutics.[3] The potential of this new class of inhibitor led us to explore compounds that bind to the novel dimer interface pocket.

RESULTS AND DISCUSSION

The 2-(quinolin-3-yl)acetic acid derivative **1** was shown to bind to the ALLINI site on HIV-1 integrase, presenting rudimentary elements of a pharmacophore that were more fully appreciated in the context of a cocrystal structure of the compound bound to the integrase CCD dimer interface.[14,15] This structure revealed a well-defined binding pocket that could accommodate small molecules and indicated the importance of both the *tert*-butoxyacetic acid moiety and the quinoline 4-substituent as key recognition elements.[14−17] The analysis of the structure focused attention on exploring alternatives to the quinoline scaffold that would offer opportunities for unique substituent vector presentation and which may lead to improved potency and enhanced drug-like properties. The initial screening strategy relied upon evaluation of test compounds in a binding assay in which displacement of a tritiated version of **1** was monitored to provide K_i values. Antiviral activity was assessed in a cell culture replication assay using a fully replicating NL_{4-3} virus containing the *Renilla* luciferase gene in place of nef (WT EC_{50}), with the cytotoxicity (CC_{50}) of test compounds toward the host MT-2 cells determined in parallel.

A computer-aided drug design (CADD) approach based on careful analysis of the cocrystal structure allowed an in silico assessment of the potential of a series of scaffolds that were scored by a best fit analysis for their complementarity to the pocket formed by the integrase dimer. To aid in this analysis, the biphenyl derivative **2** (Figure 2) was prepared as an abbreviated model system for **1** and found to be poorly active in the displacement assay with a K_i value of 67 μM, although the compound exhibited weak but detectable antiviral activity in cell culture (WT EC_{50} = 16 μM, CC_{50} = 127 μM)). Several additional scaffolds were investigated for their potential to bind to the pocket, and the pyrazolopyrimidine derivative **3** emerged as a compound with a K_i value of 2 μM in the binding assay that inhibited WT virus in cell culture with an EC_{50} value of 4.5 μM, a promising preliminary profile.

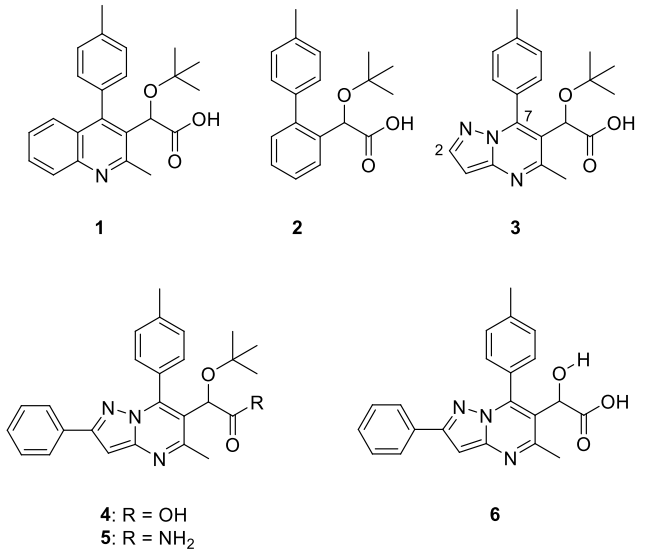

Figure 2. Scaffold modification and preliminary SAR exploration associated with ALLINIs **2**−**6**.

Structural modification of the unsaturated 6,6-fused ring system found in **1** to the 5,6-scaffold of **3** provided an alternative core system that reduced the aromatic nature of the fused heterocyclic ring while offering topologically distinct vectors for structural exploration and elaboration, particularly at the C-2 position which bisects the vectors offered by **1**. Indeed, the introduction of a phenyl substituent at the 2-position of **3** afforded **4** as a compound with improved potency in the binding assay (K_i = 700 nM) which translated to enhanced antiviral activity, WT EC_{50} = 620 nM, CC_{50} = 77 μM. Consistent with the emerging structure−activity relationships (SARs) for ALLINI inhibitors, the carboxamide **5** and alcohol **6** were considerably less potent than **4**, with WT EC_{50} values of 18 and >40 μM, respectively. As a consequence, **4** was adopted as a promising lead structure suitable for further optimization.

The initial phase of study with **4** explored the effect of variation of the C-7 substituent, with the results compiled in Table 1. Removal of the *para*-CH_3 substituent from the 7-phenyl moiety of **4** resulted in **7**, which exhibited 5-fold reduced potency in the binding assay while failing to significantly inhibit virus replication in cell culture. However, the 4-OCH_3 analogue **8** offered improved potency in the binding assay, although this compound was less active than **4** in the cell-based assay. Installation of CH_3 or OCH_3 substituents at the *meta*- and *ortho*- positions of the C-7 phenyl ring, explored in **9**-**12**, led to reduced activity in both assays. However, the incorporation of a combination of *para*-alkoxy and *meta*-alkyl substitution in the context of the chromane ring[14] of **13** resulted in a 10-fold increase in potency in the binding assay, although the magnitude did not fully translate to antiviral activity in cell culture. Substitution of the chromane ring led to the production of separable atropisomers of which the major isomer **14** was more potent than the minor isomer **15**. The identity of the atropisomers was established by single crystal X-ray structure determination which revealed **14** to be a mixture of two enantiomers, assigned as (*S*,*S*) and (*R*,*R*) (Figure 3), while **15** was a mixture of the (*S*,*R*) and (*R*,*S*) isomers (Figure 4). The separated diastereomers **14** and **15** showed no interconversion at temperatures ranging from 30

https://dx.doi.org/10.1021/acs.jmedchem.9b01681
J. Med. Chem. XXXX, XXX, XXX−XXX

Table 1. Effect of Substituent Variation at the 7-Position of Pyrazolopyrimidine 4 on Binding Potency and Antiviral Activity As Explored with 7−19

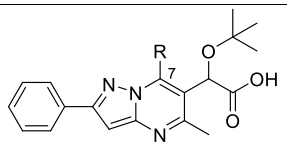

Cmpd.	R	K_i ± SD (μM)	WT EC_{50} ± SD (μM)
4	4-CH_3-C_6H_4-	0.68 ± 0.50[a]	0.62 ± 0.19[a]
7	Ph	3.7[b]	>40[b]
8	4-OCH_3-C_6H_4-	0.31 ± 0.01[a]	1.7 ± 0.16[a]
9	3-CH_3-C_6H_4-	4.4[b]	>40[b]
10	3-OCH_3-C_6H_4-	15.3[b]	>40[b]
11	2-CH_3-C_6H_4-	3.4[b]	21[b]
12	2-OCH_3-C_6H_4-	>40[b]	>40[b]
13	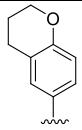	0.04 ± 0.03[a]	0.49 ± 0.24[a]
14	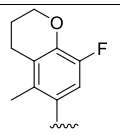 (*S*,*S* & *R*,*R*)	0.17 ± 0.09[a]	0.21 ± 0.21[a]
15	(*S*,*R* & *R*,*S*)	3.4[b]	>40[b]
16	CH_3-	>40[b]	>40[b]
17	4-CH_3-C_6H_4-NH-	>40[b]	>40[b]
18		0.43[b]	2.3[b]
19	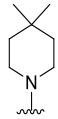	0.06 ± 0.01[a]	0.55 ± 0.04[a]

[a]K_i and EC_{50} values were the result of multiple determinations ($n \geq 2$). [b]K_i and EC_{50} values were obtained after single determinations ($n = 1$).

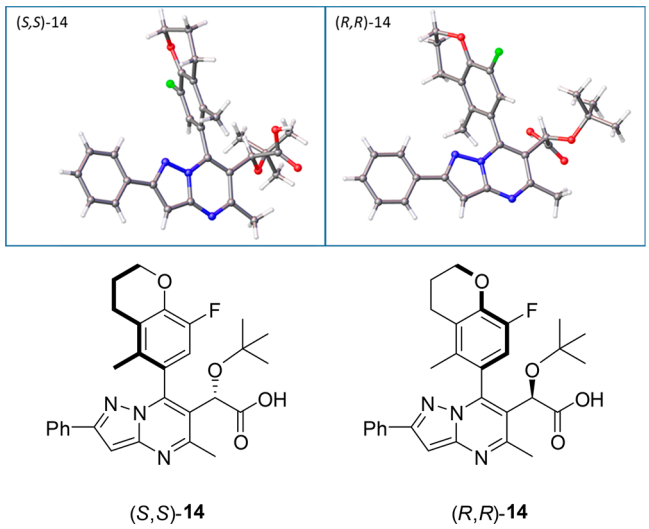

Figure 3. Single crystal X-ray structure of (*S*,*S* and *R*,*R*)-**14**.

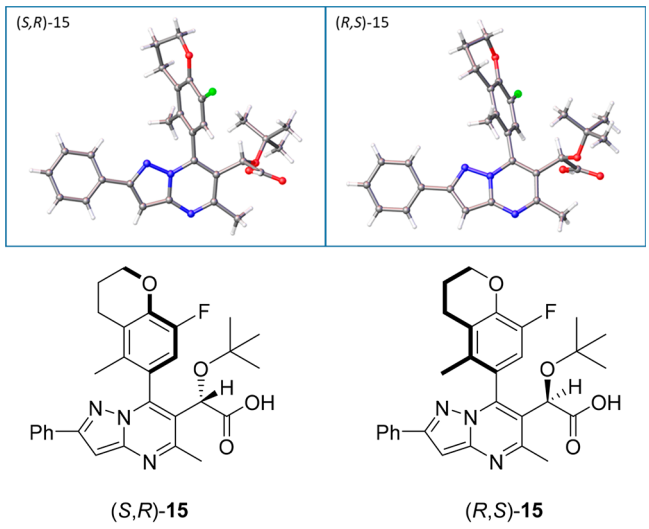

Figure 4. Single crystal X-ray structure of (*S*,*R* and *R*,*S*)-**15**.

https://dx.doi.org/10.1021/acs.jmedchem.9b01681
J. Med. Chem. XXXX, XXX, XXX−XXX

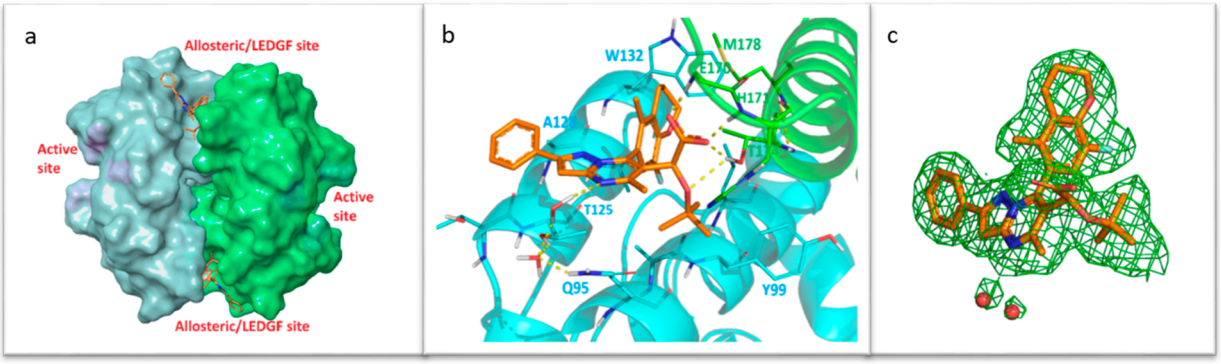

Figure 5. (a) Snapshot of the cocrystal structure of (*S*,*S*)-**14** bound to the HIV-1 integrase CCD dimer. Subunits 1 and 2 of the dimer are colored cyan and green, respectively, and (*S*,*S*)-**14** is colored orange. The catalytic domain of HIV-1 integrase that contains the DDE triad is highlighted in purple patches for comparison to the LEDGF binding site where (*S*,*S*)-**14** binds crystallographically. (b) Close-up view of the binding interactions of (*S*,*S*)-**14** in one of the two LEDGF binding pockets at the dimer interface. Hydrogen atoms were added in silico followed by a restrained minimization of the X-ray structure. (c) $F_o - F_c$ electron density map for (*S*,*S*)-**14** and surrounding water molecules contoured at 3σ.

to 100 °C in NMR experiments conducted in DMSO-d_6, with configurational stability attributed to the presence of the adjacent bulky *tert*-butoxy moiety.

Both binding and antiviral activity were dependent on the identity of the substituent at C-7, since the simple CH_3-substituted analogue **16** was poorly active in both assays, as was the substituted aniline **17**. However, cyclic amine-based substituents at C-7 were tolerated, as exemplified by **18** and **19**, with the latter compound exhibiting antiviral activity in cell culture that was comparable to **4**.

The (*S*,*S*)- and (*R*,*R*)-enantiomers of **14** were successfully separated by chromatography using a chiral column, with the (*S*,*S*)-enantiomer **14** found to be ∼100-fold more potent (K_i = 0.09 ± 0.02 μM, WT EC_{50} = 0.11 ± 0.06 μM) than the (*R*,*R*)-enantiomer (K_i > 53 μM, WT EC_{50} = 13 μM). Similarly, compound **15** was successfully resolved by chiral column chromatography; however, both enantiomers were inactive in the cell culture antiviral assay. A single crystal X-ray structure of racemic **14** (Figure 3) revealed the presence of the *S*,*S*- and *R*,*R*-enantiomers in one unit cell. In both configurations, the methyl group on the phenyl and the *tert*-butoxy group on the acid-containing side chain project in opposite directions, while the C-2 phenyl and pyrazolopyrimidine rings are coplanar and the plane of the chromane heterocycle is almost perpendicular to the core (the dihedral angle between the two planes is ∼74°). In contrast to **14**, the phenyl and the pyrazolopyrimidine elements of **15** do not approach coplanarity (Figure 4). However, the bicyclic chromane ring adopts a dihedral angle relative to the plane of the pyrimidine of ∼66°. Thus, the major difference between **14** and **15** is the conformation of the distal phenyl ring, while the elements proximal to the carboxylic acid moiety differ only slightly in their disposition.

In order to obtain further insight into the binding interactions between **14** and the enzyme, a cocrystal structure of the racemic compound and the dimeric HIV-1 integrase catalytic core domain (CCD) was determined (Figure 5). A full view of the HIV-1 integrase CCD dimer cocrystallized with two molecules of (*S*,*S*)-**14** is shown in Figure 5a. The structure demonstrated that the inhibitor occupied the same binding pocket as the LEDGF IBD and that the binding is preferential for the more potent (*S*,*S*)-enantiomer [the (*R*,*R*)-isomer was not observed]. A magnified view of one of the inhibitor binding pockets at the dimer interface is shown in Figure 5b. The carboxylic acid group of (*S*,*S*)-**14** makes a bidentate hydrogen-bonding interaction with the backbone amide NHs of Glu170 and His171 of subunit 2 of the enzyme. In addition, the side chain hydroxyl group of Thr174 of subunit 2 makes a hydrogen-bonding interaction with one of the carboxylic acid oxygen atoms. The *tert*-butoxy group occupies a hydrophobic pocket created by Thr125, Gln95, Tyr99, and Thr174, while the C7-chromane ring sculpts into another hydrophobic pocket formed by Leu102, Ala129, Thr174, Met178, Trp132, and Ala169. The interactions observed with respect to the carboxylic acid, *tert*-butoxy, and chromane moieties are consistent with what has been observed in the crystal structures of other ALLINIs bound to HIV-1 integrase CCD dimers.[18,19] The pyrazolopyrimidine core of (*S*,*S*)-**14** and the 2-phenyl substituent lie on the hydrophobic surface of the subunit 1, and the molecule exhibits tight van der Waals contact with Ala128 in the α3-helix(124−133) of subunit 1. The dihedral angle between the core heterocycle and 2-phenyl ring is ∼30°, which contrasts with the nearly coplanar arrangement observed in the single crystal X-ray structure of (*S*,*S*)-**14** (Figure 3), reflecting the conformational mobility of the substituent. An overlay of the previously solved ALLINI-bound crystal structures of HIV-1 integrase CCD dimers revealed an interesting slight shift in the α3-helix(124−133), presumably to maximize the hydrophobic contacts between Ala128 and the 2-phenyl ring of (*S*,*S*)-**14**. Two crystallographic water molecules bridge the N4 nitrogen atom of the pyrazolopyrimidine core of (*S*,*S*)-**14** with protein residues. An image of $F_o - F_c$ electron density for (*S*,*S*)-**14** and surrounding water molecules contoured at 3σ is shown in Figure 5c. Interestingly, a polyethylene glycol fragment was found to occupy a site just above the ligand. Its positioning corresponds to the positioning of the side chains of Tyr226, Trp235, and Lys266 in the carboxyl terminal domain (CTD) of the CCD−CTD interface discerned in the full length crystal structure of HIV-1 integrase solved by Gupta and colleagues.[20] Manual docking of (*S*,*S*)-**14** into this full length crystal structure of HIV-1 integrase reveals a snug fit of the 2-phenyl group in an invagination created at the CTD−CCD interface.

Comparison of the cocrystal structures of the dimeric HIV-1 integrase CCD bound to the LEDGF IBD[21] (Figure 6a) and (*S*,*S*)-**14** (Figure 5b) revealed some interesting insights into binding interactions. The carboxylic acid moiety of (*S*,*S*)-**14** engages the backbone amide groups of HIV-1 integrase via two hydrogen-bonding interactions, while the pyrazolopyrimidine

https://dx.doi.org/10.1021/acs.jmedchem.9b01681
J. Med. Chem. XXXX, XXX, XXX−XXX

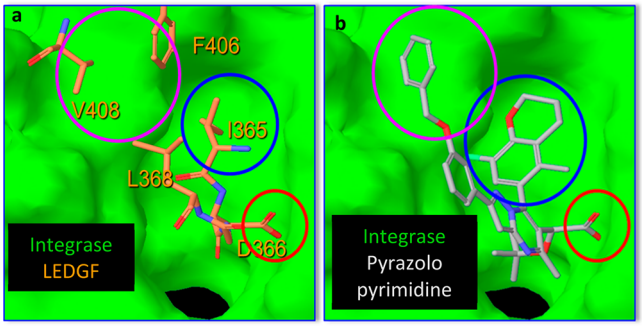

Figure 6. (a) Cocrystal structures of the dimeric HIV-1 integrase CCD bound to the LEDGF IBD. (b) Molecular modeling of substitution at the *meta*-position of the 2-phenyl group of (*S*,*S*)-**14**.

core packs into the hydrophobic pocket by relying primarily on van der Waals interactions. The carboxylic acid moiety of (*S*,*S*)-**14** mimics Asp366 of LEDGF, while the chromane group at C-7 mimics the hydrophobic side chain of Ile365. However, (*S*,*S*)-**14** does not take advantage of the interactions availed by Val408 and Phe406 in LEDGF with the integrase protein. Molecular modeling (Figure 6b) suggested that substituents at the *meta*-position of the 2-phenyl ring of (*S*,*S*)-**14** would extend deeper into the LEDGF binding pocket in a fashion that would more effectively mimic the contacts made by Val408 and Phe406 of the IBD of LEDGF. Consequently, this was viewed as a useful avenue for additional structural elaboration that may lead to improved antiviral activity and the possibility of a higher genetic barrier to the emergence of resistance.

This phase of the SAR survey is compiled in Table 2 and revealed that the judicious introduction of substituents to the 2-phenyl ring does indeed lead to enhanced antiviral activity in cell culture. The 4-CH_3 substituent in **20** improved antiviral potency by a modest 2-fold. That potency was only marginally affected by the introduction of the much larger 4-benzyloxy moiety in **21**. Further improvements were obtained with *meta*-substitutions, as explored with **22**−**24**, of which the 3-phenyl derivative **24** offered a 10-fold improvement over prototype **14**, exhibiting a WT EC_{50} value of 15 nM, CC_{50} = 10 μM. The biphenyl derivative **24** was 4-fold more potent than the phenoxy homologue **23** and comparable to the 3-benzyloxy analogue **22**. In parallel with optimization of antiviral potency, these inhibitors were profiled in a parallel artificial membrane permeability assay (PAMPA) and evaluated for metabolic stability in rat and human liver microsomal preparations. Analogues **20**−**24** exhibited uniformly high permeability in a parallel artificial membrane permeability assay (PAMPA) and generally showed good metabolic stability in the microsomal assays, suggestive of the potential to demonstrate bioavailability following oral administration.

A select set of pyrazolopyrimidines was evaluated for antiviral efficacy toward the double mutant G140S/Q148H virus strain that confers resistance to some of the active site-targeting INSTIs. GQ EC_{50} values are shown in Table 3 where the GQ mutant inhibitory activity is compared to that toward WT virus. (*S*,*S* and *R*,*R*)-**14**, (*S*,*S*)-**14**, and (*S*,*S* and *R*,*R*)-**24** fully retained potency toward the resistant virus strain, whereas the EC_{50} value for the INSTI raltegravir shifted by over 1000-fold compared to its inhibitory effect toward WT virus.

The beneficial effects of *meta*-substitutions of the C-2 phenyl moiety in **22**−**24** prompted an examination of this structural

Table 2. Effect of Structural Modification of the 2-Aryl Moiety on the Antiviral Activity, PAMPA Permeability, and Metabolic Stability in Human and Rat Liver Microsomes of Pyrazolopyrimidines 20−24 Compared to 14[f]

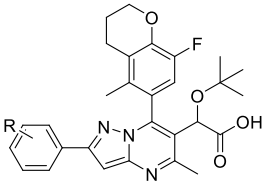

Cmpd.	R	WT EC_{50} ± SD[a] (μM)	PAMPA[c] (nm/sec)	HLM/RLM[d] (% remaining)[e]
14	H	0.21 ± 0.21	218	93/97
20	4-CH_3-	0.10 ± 0.03	492	95/94
21	4-$PhCH_2O$-	0.06 ± 0.04	313	84/79
22	3-$PhCH_2O$-	0.02 ± 0.01	570	72/83
23	3-PhO-	0.06[b]	472	100/97
24	3-Ph-	0.015 ± 0.01	652	86/100

[a]EC_{50} values were obtained by multiple determinations ($n \geq 2$). [b]EC_{50} value was obtained after a single determination ($n = 1$). [c]PAMPA values were averaged from triplicate determinations ($n = 3$). [d]HLM/RLM denotes human and rat liver microsomes, respectively. [e]Metabolic stability % remaining values were averaged from duplicate experiments ($n = 2$). [f]All compounds were screened as a mixture of the (*S*,*S*)- and (*R*,*R*)-isomers.

Table 3. Antiviral Activity of the Pyrazolopyrimidine Inhibitors against the INSTI-Resistant G140S/Q148H HIV-1 Strain (GQ EC_{50}) Compared to Raltegravir

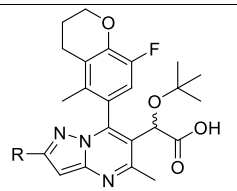

Cmpd	R	WT EC_{50} ± SD[a] (μM)	GQ EC_{50} ± SD[a] (μM)
(*S*,*S* & *R*,*R*)-**14**	C_6H_5-	0.21 ± 0.21	0.119 ± 0.03
(*S*,*S*)-**14**	C_6H_5-	0.11± 0.06	0.09[b]
(*S*,*S* & *R*,*R*)-**24**	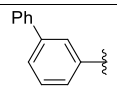	0.015 ± 0.01	0.01[b]
Raltegravir		0.002 ± 0	2.42 ± 0

[a]EC_{50} values were obtained by multiple determinations ($n \geq 2$). [b]EC_{50} value was obtained by single determination ($n = 1$).

modification in the context of the C-7 piperidine **19**, with the result that both the phenyl and benzyloxy derivatives **25** and **26**, respectively, were more potent antiviral agents (Table 4). Both **19** and **26** exhibited good PAMPA permeability and high microsomal stability in both HLM and RLM.

Several of the compounds in Tables 2 and 4 combined potent antiviral activity with good membrane permeability and high microsomal stability, which suggested that they could be

https://dx.doi.org/10.1021/acs.jmedchem.9b01681
J. Med. Chem. XXXX, XXX, XXX−XXX

Table 4. Effect of Structural Modification of the 2-Aryl Moiety on the Antiviral Activity, PAMPA Permeability, and Metabolic Stability in Human and Rat Liver Microsomes of C-7 Piperidine-Substituted Pyrazolopyrimidines 25 and 26 Compared to Prototype 19[d]

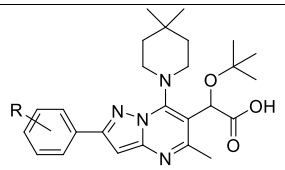

Cmpd.	R	WT EC_{50} ± SD[a] (μM)	PAMPA[b] (nm/sec)	HLM/RLM (% remaining)[c]
19	H-	0.55 ± 0.04	703	100/-
25	3-C_6H_5-	0.13 ± 0.06	-	-
26	3-$C_6H_5CH_2O$-	0.06 ± 0.02	375	100/100

[a]EC_{50} values were obtained by multiple determinations ($n \geq 2$). [b]PAMPA values were averaged from multiple replicates ($n = 3$). [c]Metabolic stability % remaining values were averaged from duplicate experiments ($n = 2$). [d]All compounds were screened as a mixture of the *S*- and R-isomers.

candidates for in vivo pharmacokinetic (PK) studies in the rat to determine the potential for exposure following oral administration. However, as a prelude to these studies, compounds were evaluated in the antiviral cell culture assay in the presence of human serum albumin (HSA EC_{50}) since these data would provide a target trough concentration of drug based on the assumption that in vivo activity would be dependent on maintaining drug levels above the protein binding-adjusted EC_{90} value. These data were obtained on the more active (*S*,*S*)-isomers. The potency of (*S*,*S*)-**24**, the prototype for the series presented in Table 5, was increased compared to the racemic mixture with an EC_{50} value of 6 nM. However, in the presence of 45 mg/mL of HSA, the approximate concentration of this plasma protein in humans, the EC_{50} value for (*S*,*S*)-**24** was 110 nM, an 18-fold attenuation. In an effort to probe this aspect of the profile of the inhibitors, analogues **27**−**31** were prepared and the (*S*,*S*)-enantiomers evaluated. As summarized in Table 5, analogues (*S*,*S*)-**27**−**31** exhibited excellent antiviral potency in the absence of HSA, with WT EC_{50} values ranging from 3 to 6 nM, while all compounds demonstrated a reduced fold-shift in the presence of HSA (5- to 6-fold) compared to (*S*,*S*)-**24**, with the notable exception of the pyridine derivative (*S*,*S*)-**30**,

Table 5. Antiviral Activity in the Absence and Presence of 45 mg/mL HSA, Fold Shift in Potency, Therapeutic Index, PAMPA Permeability, and Metabolic Stability Associated with Pyrazolopyrimidine Derivatives (*S*,*S*)-24 and (*S*,*S*)-27−31

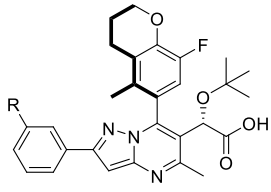

Cmpd.	R	WT EC_{50} ± SD[a] (μM)	CC_{50} ± SD[a] (μM)	TI (CC_{50}/WT EC_{50})	HSA EC_{50} ± SD[a] (μM) (45 mg/mL HSA)	Fold shift	PAMPA[c] (nm/sec)	HLM/RLM[d] (% remaining)
(*S*,*S*)-**24**	C_6H_5-	0.006 ± 0.002	6.59[b]	1098	0.11 ± 0.01	18	733	78/96
(*S*,*S*)-**27**	2-$CH_3C_6H_5$-	0.006 ± 0.002	28.15[b]	4692	0.03 ± 0.00	5	471	95/97
(*S*,*S*)-**28**	2-$CH_3OC_6H_5$-	0.006 ± 0.002	23.49 ± 9.22	3915	0.03 ± 0.01	5	765	99/99
(*S*,*S*)-**29**	2-FC_6H_5-	0.003 ± 0.001	19.08 ± 0.43	6360	0.019 ± 0.002	6	608	100/89
(*S*,*S*)-**30**	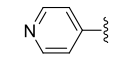	0.003 ± 0.001	13.22[b]	4406	0.07 ± 0.00	23	488	46/94
(*S*,*S*)-**31**	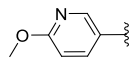	0.005 ± 0.002	>23[b]	>4600	0.023[b]	5	514	73/100
BI-224436	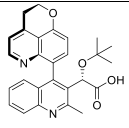	0.05± 0.02	3339.15[b]	66783	NA	NA	NA	NA

[a]EC_{50} or CC_{50} values were obtained by multiple determinations ($n \geq 2$). [b]EC_{50} or CC_{50} value was obtained by single determination ($n = 1$). [c]PAMPA values were averaged from multiple replicates ($n = 3$). [d]Metabolic stability % remaining values were averaged from duplicate experiments ($n = 2$).

https://dx.doi.org/10.1021/acs.jmedchem.9b01681
J. Med. Chem. XXXX, XXX, XXX−XXX

Table 6. Rat PK Data for (*S*,*S*)-27−29[a]

compd	C_{max} ± SD (nM)	t_{max} ± SD (h)	AUC_{0-24h} ± SD (nM·h)	$t_{1/2}$ ± SD (h)	clearance ± SD (mL min^{-1} kg^{-1})	V_{ss} ± SD (L/kg)	*F* (%)
(*S*,*S*)-**27**	1292 ± 1062	3 ± 0	6300 ± 2532	4.1 ± 0.1	7.1 ± 0.3	0.5 ± 0.1	32
(*S*,*S*)-**28**	1106 ± 697	2.3 ± 1.3	2991 ± 958	3 ± 1	28 ± 5.7	1.8 ± 1.8	59
(*S*,*S*)-**29**	803 ± 0	2.7 ± 3.8	4733 ± 0	2 ± 0	13 ± 0	0.7 ± 0.0	44

[a]All compounds were dosed at 1 mpk (iv) and 5 mpk (po). All values were obtained from multiple determinations (n = 3) for both iv and po.

Scheme 1. Synthesis of Pyrazolopyrimidine 4[a]

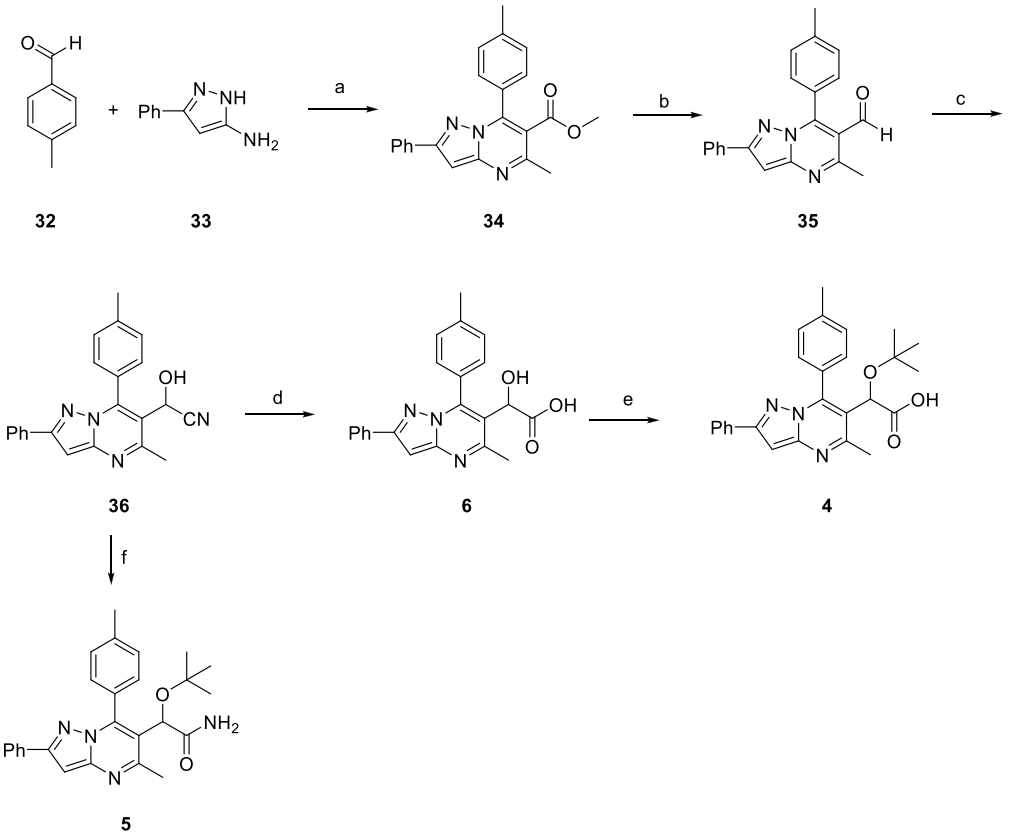

[a]Reagents and conditions: (a) (i) Methyl acetoacetate, THF, heptane, piperidine, reflux; (ii) DDQ, CH_2Cl_2; (b) (i) DIBAL, THF, CH_2Cl_2; (ii) PCC, CH_2Cl_2; (c) ZnI_2, TMSCN, CH_2Cl_2; (d) HCl (conc), 90 °C; (e) (i) $SOCl_2$, MeOH; (ii) $HClO_4$, *tert*-butyl acetate, CH_2Cl_2; (iii) LiOH, 1,4-dioxane; (f) $HClO_4$, *tert*-butyl acetate, CH_2Cl_2.

which experienced a similar ∼20-fold shift. The therapeutic index (TI) for this series of compounds is also captured in Table 5 and was found to range from 1098 to 6360, with (*S*,*S*)-**29**, one of the more potent inhibitors in the series, exhibiting a TI value of 6360, which compares with a TI value of 66 783 recorded for BI-224436[14] when tested under these assay conditions. The overall profiles of these compounds reflect a combination of good membrane permeability and reasonable metabolic stability, and those compounds with good HSA EC_{50} values, (*S*,*S*)-**27**−**29**, were advanced into rat PK studies.

Rat PK studies monitored drug levels in plasma for 24 h following oral administration of a 5 mg/kg dose. Results are compiled in Table 6. All three compounds demonstrated low to moderate clearance and low volumes of distribution. The *ortho*-methyl (*S*,*S*)-**27** and *ortho*-fluoro (*S*,*S*)-**29** derivatives exhibited lower clearance than the *ortho*-methoxy analogue (*S*,*S*)-**28**, although the latter demonstrated the highest oral bioavailability of this short series of compounds. These results indicate that the series offers promising PK profiles.

CHEMISTRY

The initial synthetic route to pyrazolopyrimidine **4** originated with the condensation of commercially available benzaldehyde **32**, 3-aminopyrazole **33**, and methyl acetoacetate in a three component, one-pot reaction that was followed by oxidation with DDQ to form the pyrazolopyrimidine core **34** (Scheme 1). The methyl ester of **34** was transformed into the aldehyde **35**, which was directly converted to the cyanohydrin **36**. *tert*-Butyl ether formation using $HClO_4$ and *tert*-butyl acetate resulted in partial hydrolysis of the nitrile moiety of **36** to give the carboxamide **5**. Alternatively, the hydrolysis of **36** under strongly acidic conditions provided the desired acid **6**. Esterification of the acid **6** and subsequent treatment with $HClO_4$ and *tert*-butyl acetate in CH_2Cl_2 installed the *tert*-butyl ether followed by saponification to yield the pyrazolopyrimidine acid **4**.

The synthetic route to access compounds with structural variation at the C-7 position is exemplified in Scheme 2 and utilized **41** as a common intermediate for C-7 modification. Reaction of aminopyrazole **33** with dimethyl 2-acetylsuccinate

https://dx.doi.org/10.1021/acs.jmedchem.9b01681
J. Med. Chem. XXXX, XXX, XXX−XXX

Scheme 2. Synthesis of Pyrazolopyrimidine 14, 15, 16, and 19[a]

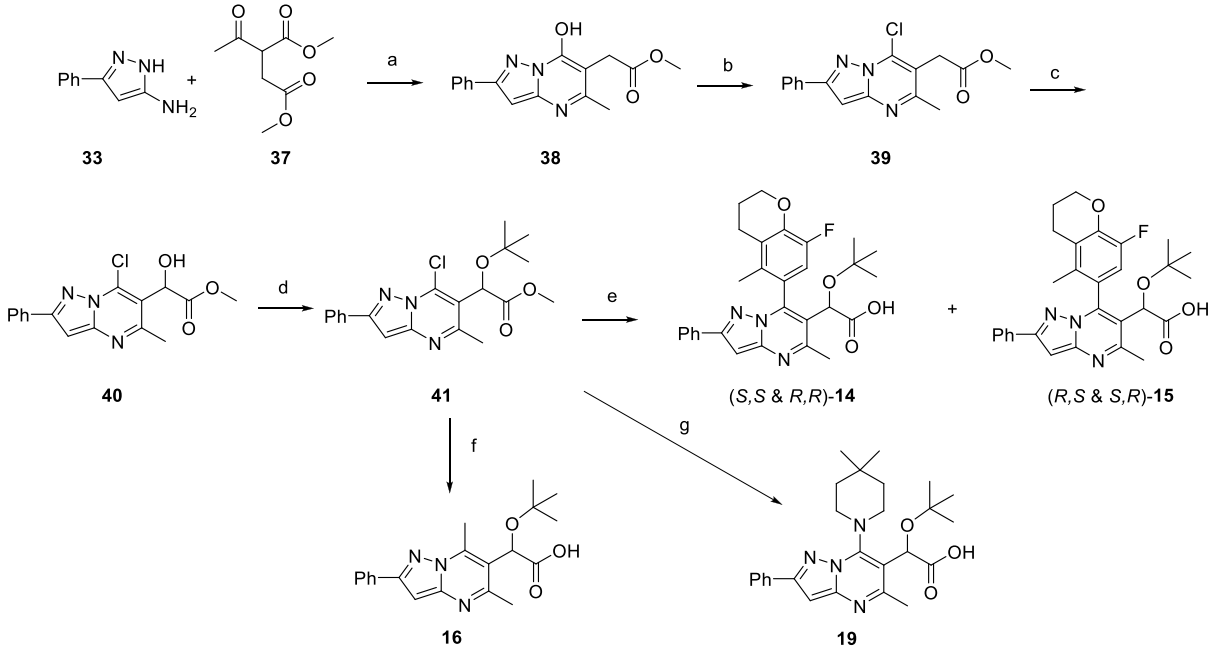

[a]Reagents and conditions: (a) *p*-TsOH·H_2O, xylene, reflux; (b) $POCl_3$, reflux; (c) (i) KHMDS, THF, −78 °C; (ii) 2-(phenylsulfonyl)-3-phenyloxaziridine (Davis reagent); (d) $HClO_4$, *tert*-butylacetate, CH_2Cl_2; (e) (i) 2-(8-fluoro-5-methylchroman-6-yl)-4,4,5,5-tetramethyl-1,3,2-dioxaborolane, $Pd(PPh_3)_4$, K_2CO_3, DMF, microwave, 130 °C; (ii) LiOH, 1,4-dioxane; (f) (i) $Pd(PPh_3)_4$, MeZnCl, THF; (ii) LiOH, 1,4-dioxane; (g) (i) 4,4-dimethylpiperidine, HCl salt, DIEA, NMP, 50 °C; (ii) LiOH.

Scheme 3. Synthesis of Pyrazolopyrimidine (*S,S*)- and (*R,R*)-20 and -25[a]

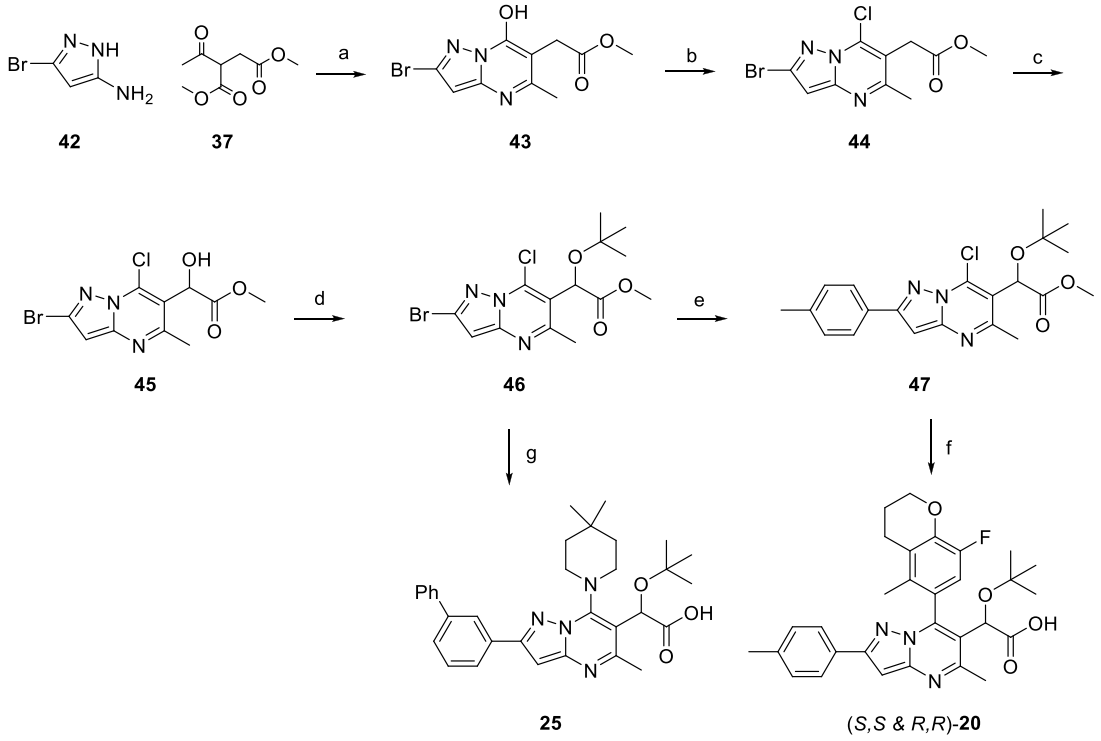

[a]Reagents and conditions: (a) *p*-TsOH·H_2O, xylene, reflux; (b) $POCl_3$, reflux; (c) (i) KHMDS, THF, −78 °C; (ii) 2-(phenylsulfonyl)-3-phenyloxaziridine (Davis reagent); (d) $HClO_4$, *tert*-butyl acetate, DCM; (e) (i) *p*-tolylboronic acid, $Pd(PPh_3)_4$, K_2CO_3 (2M), DMF, microwave, 70 °C; (f) (i) 2-(8-fluoro-5-methylchroman-6-yl)-4,4,5,5-tetramethyl-1,3,2-dioxaborolane, $Pd(PPh_3)_4$, K_3PO_4 (2M), DMF, microwave, 130 °C; (ii) LiOH 1,4-dioxane; (g) (i) 2-([1,1′-biphenyl]-3-yl)-4,4,5,5-tetramethyl-1,3,2-dioxaborolane, $Pd(PPh_3)_4$, K_2CO_3 (2 M), DMF, microwave, 70 °C; (ii) 4,4-dimethylpiperidine, HCl salt, DIEA, NMP, 50 °C; (iii) LiOH, 1,4-dioxane.

https://dx.doi.org/10.1021/acs.jmedchem.9b01681
J. Med. Chem. XXXX, XXX, XXX−XXX

Scheme 4. Chiral Synthesis of Pyrazolopyrimidine (*S*,*S*)-27[a]

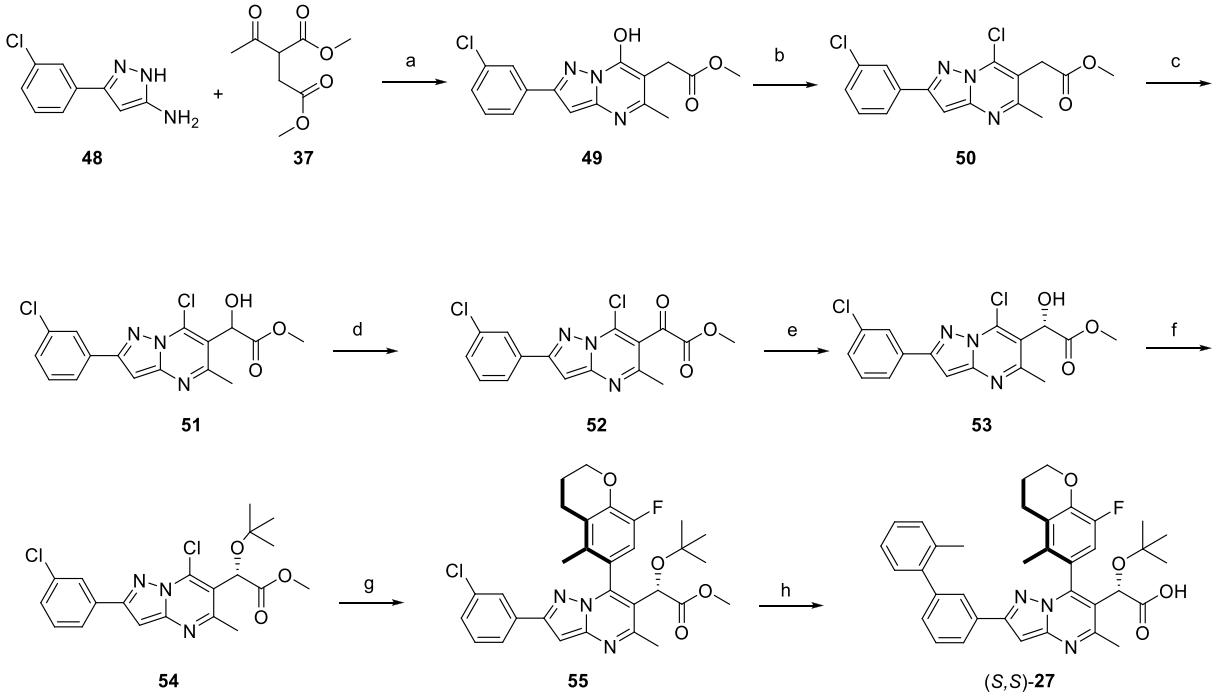

[a]Reagents and conditions: (a) *p*-TsOH·H_2O, xylene, reflux; (b) $POCl_3$, reflux; (c) (i) KHMDS, THF, −78 °C; (ii) 2-(phenylsulfonyl)-3-phenyloxaziridine (Davis reagent); (d) Dess−Martin periodinane, CH_2Cl_2; (e) (*R*)-1-methyl-3,3-diphenyltetrahydro-1*H*,3*H*-pyrrolo[1,2-*c*][1,3,2]oxazaborole, catecholborane, toluene; (f) $HClO_4$, *tert*-butyl acetate, CH_2Cl_2; (g) 2-(8-fluoro-5-methylchroman-6-yl)-4,4,5,5-tetramethyl-1,3,2-dioxaborolane, $Pd(PPh_3)_4$, K_3PO_4 (2 M), DMF, microwave, 130 °C; (h) (i) *o*-tolylboronic acid, $Pd(OAc)_2$, S-Phos, K_3PO_4 (2M), DMF, microwave, 130 °C; (ii) LiOH, 1,4-dioxane.

(**37**) afforded pyrazolopyrimidine **38**, which was converted to the chloride **39** using $POCl_3$. The benzylic hydroxyl group on **40** was introduced by deprotonation followed by treatment with the Davis reagent[22] to give **40** as a racemic mixture. Alcohol **40** was treated with $HClO_4$ and *tert*-butyl acetate in CH_2Cl_2 to afford the *tert*-butyl ether **41**, a versatile intermediate. Subjecting **41** to a Suzuki−Miyaura coupling at C-7 with arylboronic acids allowed the introduction of a diverse set of aryl substituents. A Negishi coupling reaction was used to introduce C-7 alkyl groups, while a nucleophilic displacement reaction with different amines or anilines resulted in a series of C-7 amino-substituted analogs.

An alternative synthetic route was developed to introduce modifications at C-2 and began with condensation of 5-bromo-3-aminopyrazole (**42**) with **37** afforded pyrazolopyrimidine **43**, which was converted to the chloride **44** using $POCl_3$. The benzylic hydroxyl group on **45** was introduced by deprotonation followed by treatment with Davis reagent to give **45** as a racemic mixture. Alcohol **45** was then treated with $HClO_4$ and *t*-butyl acetate in CH_2Cl_2 to procure the key intermediate **46** (Scheme 3). A selective Suzuki−Miyaura coupling at the C-2 position of **46** was realized by controlling the reaction temperature and varying the base (70 °C, K_2CO_3). After completion of the Suzuki−Miyaura coupling at the 2-position, the 7-chloro was subjected to a second Suzuki−Miyaura coupling that was conducted at 130 °C using K_3PO_4 as the base. Alternatively, the C-7 chlorine could be displaced by amines. A final hydrolysis afforded acids **20** and **25**.

Although the active chiral compound (*S*,*S*)-**14** and the less active enantiomer (*R*,*R*)-**14** could be separated by chiral column chromatography, the yield of the active enantiomer was low and the separation was time-consuming. To alleviate this problem, an efficient chiral synthetic route was developed to make the (*S*,*S*)-isomer of the biarylpyrazolopyrimidines starting from aminopyrazole **48** (Scheme 4). The racemic alcohol **51** was oxidized to the corresponding ketone using the Dess−Martin reagent, setting the stage for an enantioselective reduction using catecholborane in the presence of a chiral oxazaborolidine,[23] which resulted in the isolation of (*S*)-**53** with 96% ee. Compound **53** was treated with $HClO_4$ and *tert*-butyl acetate to afford the corresponding *tert*-butyl ether **54**, which was subjected to two consecutive Suzuki−Miyaura coupling reactions. The phenyl-based chlorine is much less reactive than the chlorine attached to the pyrimidine ring, allowing for excellent selectivity and directing the first Suzuki−Miyaura coupling to C-7. The second Suzuki−Miyaura coupling was achieved in the presence of $Pd(OAc)_2$ using the S-Phos ligand, and hydrolysis of **55** gave the targeted chiral pyrazolopyrimidine (*S*,*S*)-**27**.

CONCLUSION

This manuscript describes the design, synthesis, and biological activities of a series of novel pyrazolopyrimidines that act as potent allosteric inhibitors of HIV-1 integrase and exhibit drug-like properties. Separation, characterization, and screening of four diastereomers (*S*,*S*)-**14**, (*R*,*R*)-**14**, (*S*,*R*)-**15**, and (*R*,*S*)-**15** provided interesting SARs and demonstrated an impact of conformational differences between atropisomers. A cocrystal structure of (*S*,*S*)-**14** with the dimeric HIV-1 integrase CCD revealed that the inhibitor occupied the same binding pocket as LEDGF. Molecular modeling based on the crystal structure data predicted that substituents incorporated at the *meta*-

https://dx.doi.org/10.1021/acs.jmedchem.9b01681
J. Med. Chem. XXXX, XXX, XXX−XXX

position of 2-phenyl group would extend deeper into the ALLINI binding pocket, modifications postulated to lead to increased binding affinity and antiviral activity. This vector proved to be a useful avenue for structural elaboration and resulted in inhibitors with excellent antiviral activity in cell culture. The most potent compound **29** exhibited a WT EC_{50} value of 0.003 μM, while **26**, which incorporates a dimethylpiperidine substituent at the 7- position, resulted in a WT EC_{50} value of 0.06 μM. Both the vector on the 2-position and the amino substituent at the 7-position of the core offer unique SARs for allosteric integrase inhibitors, unprecedented based on prior patent publications[24] and literature articles.[14,16,17] Three compounds, **27**−**29**, that exhibited good overall profiles in the in vitro antiviral and PK screening assays, including minimal potency shifts in the presence of HSA, were advanced into rat PK studies and showed promising PK profiles with good oral bioavailability. Further studies based on this chemotype led to allosteric HIV-1 IN inhibitors with excellent cellular potency.[25]

EXPERIMENTAL SECTION

Chemistry Information. Solvents and reagents were used directly as obtained from commercial sources. Flash chromatography was performed on silica gel 60 (0.040−0.063 particle size; EM Science supply). ^{1}H NMR spectra were recorded on a Bruker DRX-500f spectrometer at 500 MHz (or Bruker AV 400 MHz, Bruker DPX-300B, or Varian Gemini 300 at 300 MHz as stated). The chemical shifts are reported in ppm on the δ scale relative to δTMS = 0. The following internal references were used for the residual protons in the following solvents: $CDCl_3$ (δ_H 7.26), CD_3OD (δ_H 3.30), acetic-d_4 (acetic acid-d_4) (δ_H 11.6, 2.07), DMSOmix or DMSO-d_6 $CDCl_3$ (δ_H 2.50 and 8.25) (ratio 75%:25%), and DMSO-d_6 (δ_H 2.50). Standard abbreviations were employed to describe the multiplicity patterns: s (singlet), br s (broad singlet), d (doublet), t (triplet), q (quartet), m (multiplet), b (broad), app (apparent). The coupling constants (J) are reported in hertz. All liquid chromatography (LC) data were recorded on a Shimadzu LC-10AS liquid chromatograph using a SPD-10AV UV−vis detector with mass spectrometry (MS) data determined using a Micromass Platform for LC in electrospray mode. The purity of the final compounds was determined by HPLC as described above and is 95% or higher unless specified otherwise.

2-(*tert*-Butoxy)-2-(4′-methyl-[1,1′-biphenyl]-2-yl)acetic Acid (2). Di-*tert*-butyl dicarbonate (4.453 g, 20.40 mmol) was added to a mixture of methyl 2-(2-bromophenyl)-2-hydroxyacetate (2000 mg, 8.16 mmol), $Mg(ClO_4)_2$ (273 mg, 1.224 mmol) in CH_2Cl_2 (12 mL) and stirred for 72 h at room temperature. The solvent was evaporated and the residue purified by silica gel chromatography to provide methyl 2-(2-bromophenyl)-2-(*tert*-butoxy)acetate (1000 g, 40.7%). ^{1}H NMR (400 MHz, $CDCl_3$) δ (ppm): 7.66 (d, 2H), 7.54 (d, 2H), 7.36−7.15 (m, 2 H), 6.93 (s, 1 H), 5.50 (s, 1 H), 3.70 (s, 3 H), 1.25 (s, 9 H). MS ($C_{13}H_{17}BrO_3$): m/z 323 (M + Na)$^+$. A mixture of methyl 2-(2-bromophenyl)-2-(*tert*-butoxy)acetate (30 mg, 0.100 mmol), *p*-tolylboronic acid (20.3 mg, 0.149 mmol), $Pd(Ph_3P)_4$ (17.3 mg, 0.015 mmol), 2 M K_3PO_4 (200 μL) in DMF (2 mL) was heated in a microwave reactor at 130 °C for 10 min. The reaction mixture was filtered and the filtrate was purified by preparative HPLC to give methyl 2-(*tert*-butoxy)-2-(4′-methyl-[1,1′-biphenyl]-2-yl)-acetate (22 mg, 70.7%). ^{1}H NMR (400 MHz, MeOD) δ (ppm): 7.58−7.56 (m, 1 H), 7.36−7.20 (m, 7 H), 5.24 (s, 1 H), 3.68 (s, 3 H), 2.42 (s, 3 H), 0.95 (s, 9 H). MS ($C_{20}H_{24}O_3$): m/z 335 (M + Na)$^+$. 1 N LiOH aqueous solution (0.6 mL, 0.6 mmol was added to a solution of methyl 2-(*tert*-butoxy)-2-(4′-methyl-[1,1′-biphenyl]-2-yl)acetate (22 mg, 0.070 mmol) in dioxane (0.6 mL), and the mixture was stirred at room temperature for 2 h. The reaction mixture was filtered and the filtrate was purified by preparative HPLC to afford **2** (15.7 mg, 74.0%). ^{1}H NMR (400 MHz, MeOD) δ (ppm): 7.60−7.58 (m, 1 H), 7.38−7.22 (m, 7 H), 5.22 (s, 1 H), 2.42 (s, 3 H), 0.93 (s, 9 H). MS ($C_{19}H_{22}O_3$): m/z 321 (M + Na)$^+$.

2-*tert*-Butoxy-2-(5-methyl-7-*p*-tolylpyrazolo[1,5-*a*]-pyrimidin-6-yl)acetic Acid, TFA Salt (3). Compound **3** was prepared from 1*H*-pyrazol-3-amine in a manner similar to that described for compound **4**. ^{1}H NMR (500 MHz, MeOD) δ (ppm): 8.03 (d, J = 2.4 Hz, 1H), 7.66−7.42 (m, 4 H), 6.63 (d, J = 2.4 Hz, 1H), 5.16 (s, 1 H), 2.70 (s, 3 H), 2.52 (s, 3 H), 0.98 (s, 9 H). MS ($C_{20}H_{23}N_3O_3$): m/z 354 (M + H)$^+$. HRMS calcd for $C_{20}H_{23}N_3O_3$ 354.1812 (MH^+); found 354.1819.

2-*tert*-Butoxy-2-(5-methyl-2-phenyl-7-*p*-tolylpyrazolo[1,5-*a*]pyrimidin-6-yl)acetic Acid, TFA Salt (4). $SOCl_2$ (0.0023 mL, 0.032 mmol) was added to a solution of **6** (6 mg, 0.016 mmol) in MeOH (2 mL) and the reaction mixture stirred at 40 °C for 16 h. The solvent was evaporated to give methyl 2-hydroxy-2-(5-methyl-2-phenyl-7-*p*-tolylpyrazolo[1,5-*a*]pyrimidin-6-yl)acetate. The crude product was used directly for next step. MS ($C_{23}H_{21}N_3O_3$): m/z 388 (M + H)$^+$. Perchloric acid (0.008 mL, 0.128 mmol) was added to a solution of methyl 2-hydroxy-2-(5-methyl-2-phenyl-7-*p*-tolylpyrazolo[1,5-*a*]pyrimidin-6-yl)acetate (6.20 mg, 0.016 mmol) in *tert*-butyl acetate (0.3 mL) and the reaction mixture stirred for 2 h at room temperature. The reaction mixture was quenched with H_2O and diluted with EtOAc. The organic phase was washed with saturated $NaHCO_3$ and dried over Na_2SO_4. The solvent was evaporated to give methyl 2-*tert*-butoxy-2-(5-methyl-2-phenyl-7-*p*-tolylpyrazolo[1,5-*a*]-pyrimidin-6-yl)acetate. The crude product was used directly for the next step. MS ($C_{27}H_{29}N_3O_3$): m/z 444 (M + H)$^+$. 1.5 N LiOH aqueous solution (0.5 mL, 0.750 mmol) was added to a solution of methyl 2-*tert*-butoxy-2-(5-methyl-2-phenyl-7-*p*-tolylpyrazolo[1,5-*a*]-pyrimidin-6-yl)acetate (7.10 mg, 0.016 mmol) in dioxane (0.5 mL) and the mixture stirred at 50 °C for 2 h. The reaction mixture was filtered and the filtrate was purified by preparative HPLC to afford **4** as TFA salt (4 mg, 43.7% for 3 steps). ^{1}H NMR (400 MHz, MeOD) δ (ppm): 7.91−7.82 (m, 2 H), 7.67 (dd, J = 7.8, 2.8 Hz, 2H), 7.49 (d, J = 8.0 Hz, 2H), 7.43−7.28 (m, 3 H), 6.94 (s, 1 H), 5.19 (s, 1 H), 2.69 (s, 3 H), 2.53 (s, 3 H), 0.97 (s, 9 H). MS ($C_{26}H_{27}N_3O_3$): m/z 430 (M + H)$^+$.

2-(*tert*-Butoxy)-2-(5-methyl-2-phenyl-7-(*p*-tolyl)pyrazolo-[1,5-*a*]pyrimidin-6-yl)acetamide, TFA Salt (5). Perchloric acid (0.008 mL, 0.128 mmol) was added to a solution of **36** (3 mg, 8.46 μmol) in *tert*-butyl acetate (0.3 mL) and the mixture stirred for 3 h at room temperature. The reaction mixture was quenched with H_2O and diluted with EtOAc. The solvent was evaporated and the residue was purified by preparative HPLC to afford **5** as TFA salt (2 mg, 52.4%). ^{1}H NMR (400 MHz, MeOD) δ (ppm): 7.87−7.85 (m, 2 H), 7.62−7.58 (m, 2 H), 7.45−7.36 (m, 5 H), 6.93 (s, 1 H), 5.05 (s, 1 H), 2.66 (s, 3 H), 2.50 (s, 3 H), 1.40 (s, 9 H). MS ($C_{26}H_{28}N_4O_2$): m/z 429 (M + H)$^+$.

2-Hydroxy-2-(5-methyl-2-phenyl-7-*p*-tolylpyrazolo[1,5-*a*]-pyrimidin-6-yl)acetic Acid (6). A solution of **36** (28 mg, 0.079 mmol) in conc HCl (400 μL, 4.87 mmol) was heated at 90 °C for 3 h. The solvent was evaporated and the residue was purified by preparative HPLC to afford **6** (14 mg, 47.5%). ^{1}H NMR (400 MHz, MeOD) δ (ppm): 7.93−7.80 (m, 2 H), 7.57 (d, J = 8.3 Hz, 2H), 7.51−7.29 (m, 5 H), 6.95 (s, 1 H), 5.19 (s, 1 H), 2.67 (s, 3 H), 2.51 (s, 3 H). MS ($C_{22}H_{19}N_3O_3$): m/z 374 (M + H)$^+$.

2-(*tert*-Butoxy)-2-(5-methyl-2,7-diphenylpyrazolo[1,5-*a*]-pyrimidin-6-yl)acetic Acid (7). The title compound was prepared from methyl 2-*tert*-butoxy-2-(7-chloro-5-methyl-2-phenylpyrazolo-[1,5-*a*]pyrimidin-6-yl)acetate in a manner similar to that described for **14**. ^{1}H NMR (600 MHz, DMSO/$CDCl_3$) δ (ppm): 7.84 (d, J = 7.6 Hz, 2H), 7.76−7.67 (m, 5 H), 7.42−7.34 (m, 3 H), 7.06 (s, 1 H), 4.97 (s, 1 H), 2.53 (s, 3 H), 0.91 (s, 9 H). MS ($C_{25}H_{25}N_3O_3$): m/z 416 (M + H)$^+$.

2-(*tert*-Butoxy)-2-(7-(4-methoxyphenyl)-5-methyl-2-phenylpyrazolo[1,5-*a*]pyrimidin-6-yl)acetic Acid, TFA Salt (8). The title compound was prepared from methyl 2-*tert*-butoxy-2-(7-chloro-5-methyl-2-phenylpyrazolo[1,5-*a*]pyrimidin-6-yl)acetate in a manner similar to that described for **14**. ^{1}H NMR (600 MHz, DMSO/$CDCl_3$) δ (ppm): 7.86 (d, J = 8.2 Hz, 2H), 7.75−7.65 (m, 2

https://dx.doi.org/10.1021/acs.jmedchem.9b01681
J. Med. Chem. XXXX, XXX, XXX−XXX

H), 7.43−7.35 (m, 3 H), 7.20 (d, J = 8.8 Hz, 2H), 7.03 (s, 1 H), 5.05 (s, 1 H), 3.92 (s, 3 H), 2.53 (s, 3 H), 0.92 (s, 9 H). MS ($C_{26}H_{27}N_3O_4$): m/z 446 (M + H)$^+$.

2-(*tert*-Butoxy)-2-(5-methyl-2-phenyl-7-(*m*-tolyl)pyrazolo-[1,5-*a*]pyrimidin-6-yl)acetic Acid (9). The title compound was prepared from methyl 2-*tert*-butoxy-2-(7-chloro-5-methyl-2-phenylpyrazolo[1,5-*a*]pyrimidin-6-yl)acetate in a manner similar to that described for **14**. ^{1}H NMR (600 MHz, DMSO/$CDCl_3$) δ (ppm): 7.84 (d, J = 7.0 Hz, 2H), 7.55−7.47 (m, 4 H), 7.44−7.35 (m, 3 H), 7.05 (s, 1 H), 4.97 (s, 1 H), 2.53 (s, 3 H), 2.45 (s, 3 H), 0.92 (s, 9 H). MS ($C_{26}H_{27}N_3O_3$): m/z 430 (M + H)$^+$.

2-(*tert*-Butoxy)-2-(7-(3-methoxyphenyl)-5-methyl-2-phenylpyrazolo[1,5-*a*]pyrimidin-6-yl)acetic Acid (10). The title compound was prepared from methyl 2-*tert*-butoxy-2-(7-chloro-5-methyl-2-phenylpyrazolo[1,5-*a*]pyrimidin-6-yl)acetate in a manner similar to that described for **14**. ^{1}H NMR (600 MHz, DMSO/$CDCl_3$) δ (ppm): 7.85 (d, J = 7.0 Hz, 2H), 7.59−7.56 (m, 1 H), 7.42−7.21 (m, 6 H), 7.05 (s, 1 H), 5.02 (s, 1 H), 3.84 (s, 3 H), 2.53 (s, 3 H), 0.93 (s, 9 H). MS ($C_{26}H_{27}N_3O_4$): m/z 446 (M + H)$^+$.

2-(*tert*-Butoxy)-2-(5-methyl-2-phenyl-7-(*o*-tolyl)pyrazolo-[1,5-*a*]pyrimidin-6-yl)acetic Acid (11). The title compound was prepared from methyl 2-*tert*-butoxy-2-(7-chloro-5-methyl-2-phenylpyrazolo[1,5-*a*]pyrimidin-6-yl)acetate in a manner similar to that described for **14**. ^{1}H NMR (600 MHz, DMSO/$CDCl_3$) δ (ppm): 7.79 (d, J = 7.6 Hz, 2H), 7.54−7.46 (m, 2 H), 7.41−7.33 (m, 5 H), 7.04 (s, 1 H), 4.81 (s, 1 H), 2.73 (s, 3 H), 2.53 (s, 3 H), 1.11 (s, 9 H). MS ($C_{26}H_{27}N_3O_3$): m/z 430 (M + H)$^+$.

2-(*tert*-Butoxy)-2-(7-(2-methoxyphenyl)-5-methyl-2-phenylpyrazolo[1,5-*a*]pyrimidin-6-yl)acetic Acid (12). The title compound was prepared from methyl 2-*tert*-butoxy-2-(7-chloro-5-methyl-2-phenylpyrazolo[1,5-*a*]pyrimidin-6-yl)acetate in a manner similar to that described for **14**. ^{1}H NMR (600 MHz, DMSO/$CDCl_3$) δ (ppm): 7.82 (d, J = 7.6 Hz, 2H), 7.67−7.64 (m, 1 H), 7.52−7.18 (m, 6 H), 7.00 (s, 1 H), 4.94 (s, 1 H), 3.68 (s, 3 H), 2.53 (s, 3 H), 0.94 (s, 9 H). MS ($C_{26}H_{27}N_3O_4$): m/z 446 (M + H)$^+$.

2-(*tert*-Butoxy)-2-(7-(chroman-6-yl)-5-methyl-2-phenylpyrazolo[1,5-*a*]pyrimidin-6-yl)acetic Acid (13). The title compound was prepared from methyl 2-*tert*-butoxy-2-(7-chloro-5-methyl-2-phenylpyrazolo[1,5-*a*]pyrimidin-6-yl)acetate in a manner similar to that described for **14**. ^{1}H NMR (600 MHz, DMSO/$CDCl_3$) δ (ppm): 7.96 (s, 1H), 7.87 (d, J = 7.0 Hz, 2H), 7.60−7.30 (m, 4 H), 7.02 (s, 1 H), 6.98 (d, J = 8.8 Hz, 1H), 5.07 (s, 1 H), 4.29 (br s, 2H), 2.84 (s, 2H), 2.61 (s, 3 H), 2.04 (br s, 2H), 0.93 (9 H, s). MS ($C_{28}H_{29}N_3O_4$): m/z 472 (M + H)$^+$.

2-(*tert*-Butoxy)-2-(7-(8-fluoro-5-methylchroman-6-yl)-5-methyl-2-phenylpyrazolo[1,5-*a*]pyrimidin-6-yl)acetic Acid, TFA Salt (*S,S* and *R,R*)-14 and (*S,R* and *R,S*)-15. A mixture of **41** (50 mg, 0.1 mmol), $Pd(PPh_3)_4$ (17.27 mg, 0.015 mmol), 2-(8-fluoro-5-methylchroman-6-yl)-4,4,5,5-tetramethyl-1,3,2-dioxaborolane (58.2 mg, 0.199 mmol), and 2 M K_3PO_4 solution (300 μL) in DMF (4 mL) was heated in a microwave reactor at 130 °C for 15 min. The reaction mixture was filtered and the filtrate purified by preparative HPLC to afford (*S,S* and *R,R*)-methyl 2-(*tert*-butoxy)-2-(7-(8-fluoro-5-methylchroman-6-yl)-5-methyl-2-phenylpyrazolo[1,5-*a*]pyrimidin-6-yl)acetate (30 mg, 54.3%) and (*S,R* and *R,S*) isomer (1.6 mg, 2.9%) as TFA salt. (*S,S* and *R,R*)-Methyl 2-(*tert*-butoxy)-2-(7-(8-fluoro-5-methylchroman-6-yl)-5-methyl-2-phenylpyrazolo[1,5-*a*]pyrimidin-6-yl)acetate. ^{1}H NMR (400 MHz, CD_3OD) δ (ppm): 7.83 (dd, J = 8.2, 1.6 Hz, 2H), 7.48−7.27 (m, 3 H), 7.04−6.85 (m, 2 H), 5.08 (s, 1 H), 4.33−4.30 (m, 2 H), 3.68 (s, 3 H), 2.81 (t, J = 6.5 Hz, 2H), 2.75 (s, 3 H), 2.20−2.14 (m, 2 H), 1.87 (s, 3 H), 1.17 (s, 9 H). MS ($C_{30}H_{32}FN_3O_4$): m/z 518 (M + H)$^+$. (*S,R* and *R,S*)-Methyl 2-(*tert*-butoxy)-2-(7-(8-fluoro-5-methylchroman-6-yl)-5-methyl-2-phenylpyrazolo[1,5-*a*]pyrimidin-6-yl)acetate. MS ($C_{30}H_{32}FN_3O_4$): m/z 518 (M + H)$^+$. Hydrolysis of these esters as described for **4** gave the title compounds (*S,S* and *R,R*)-**14** and (*S,R* and *R,S*)-**15**. (*S,S* and *R,R*)-**14**. ^{1}H NMR (500 MHz, CD_3OD) δ (ppm): 7.83 (d, J = 7.2 Hz, 2H), 7.42−7.34 (m, 3H), 6.96 (d, J = 10.99 Hz, 1H), 6.90 (s, 1H), 4.58 (s, 1H), 4.41−4.23 (m, 2H), 2.85−2.80 (m, 5H), 2.18−2.14 (m, 2H), 1.97 (s, 3H), 1.17 (s, 9H). MS ($C_{29}H_{30}FN_3O_4$): m/z 504 (M + H)$^+$. (*S,R* and *R,S*)-**15**. ^{1}H NMR (300 MHz, DMSO-d_6) δ (ppm): 13.26 (br s, 1H), 7.87 (d, J = 7.4 Hz, 2H), 7.49−7.37 (m, 3H), 7.20 (d, J = 11.2 Hz, 1H), 7.14 (s, 1H), 4.93 (s, 1H), 4.24−4.38 (m, 2H), 2.84−2.66 (m, 2H), 2.64 (s, 3H, s), 2.16−2.04 (m, 2H), 1.78 (s, 3H), 0.96 (s, 9H). MS ($C_{29}H_{30}FN_3O_4$): m/z 504 (M + H)$^+$. Single crystal structures for (*S,S* and *R,R*)-**14** and (*S,R* and *R,S*)-**15** have been deposited in the CCDC database under CCDC deposition numbers 1862636 and 1862637, respectively.

2-*tert*-Butoxy-2-(7-(8-fluoro-5-methylchroman-6-yl)-5-methyl-2-phenylpyrazolo[1,5-*a*]pyrimidin-6-yl)acetic Acid (*S,S*)-14 and 2-*tert*-butoxy-2-(7-(8-fluoro-5-methylchroman-6-yl)-5-methyl-2-phenylpyrazolo[1,5-*a*]pyrimidin-6-yl)acetic Acid (*R,R*)-14. The title compounds were synthesized using a two-step method starting from the racemic ester precursor for compound (*S,S* and *R,R*)-**14**. The racemic ester was separated into two enantiomers using a chiral column to give (*S,S*)-methyl 2-*tert*-butoxy-2-(7-(8-fluoro-5-methylchroman-6-yl)-5-methyl-2-phenylpyrazolo[1,5-*a*]pyrimidin-6-yl)acetate and (*R,R*)-methyl 2-*tert*-butoxy-2-(7-(8-fluoro-5-methylchroman-6-yl)-5-methyl-2-phenylpyrazolo[1,5-*a*]pyrimidin-6-yl)acetate. Chiral separation method: Chiralpak AD-H preparative column, 20 mm × 250 mm, 5 μm. Mobile phase: 15% MeOH in CO_2 at 150 bar. Temp: 35 °C. Flow rate: 45.0 mL/min for 14 min. UV was monitored at 254 nm. Hydrolysis of these esters as described for compound **4** gave the title compounds (*S,S*)-**14** and (*R,R*)-**14**.

2-*tert*-Butoxy-2-(5,7-dimethyl-2-phenylpyrazolo[1,5-*a*]-pyrimidin-6-yl)acetic Acid, TFA Salt (16). A mixture of **41** (20 mg, 0.052 mmol), $Pd(PPh_3)_4$ (20 mg, 0.017 mmol), methylzinc(II) chloride (0.5 mL, 1.000 mmol), and THF (0.8 mL) was heated in a microwave reactor at 130 °C for 15 min. The reaction mixture was quenched with H_2O, extracted with EtOAc, and the combined organic layer was dried over anhydrous Na_2SO_4, filtered, and concentrated. The residue was purified by preparative HPLC to give methyl 2-*tert*-butoxy-2-(5,7-dimethyl-2-phenylpyrazolo[1,5-*a*]pyrimidin-6-yl)-acetate as the TFA salt (15 mg, 60.4%). ^{1}H NMR (400 MHz, $CDCl_3$) δ (ppm): 8.04−8.02 (m, 2 H), 7.56−7.38 (m, 3 H), 7.06 (s, 1 H), 5.41 (s, 1 H), 3.75 (s, 3 H), 3.10 (s, 3 H), 2.85 (s, 3 H), 1.28 (s, 9 H). MS ($C_{21}H_{25}N_3O_3$): m/z 368 (M + H)$^+$. An aqueous solution of 1.5 N LiOH (0.5 mL, 0.750 mmol) was added to a solution of the TFA salt of methyl 2-*tert*-butoxy-2-(5,7-dimethyl-2-phenylpyrazolo[1,5-*a*]-pyrimidin-6-yl)acetate (15 mg, 0.031 mmol) in dioxane (0.5 mL) and the mixture stirred at room temperature for 4 h. The reaction mixture was filtered and the filtrate was purified by preparative HPLC to afford the TFA salt of **16** (13 mg, 89%). ^{1}H NMR (500 MHz, $CDCl_3$) δ (ppm): 9.92 (br s, 1H), 8.06−7.89 (m, 2 H), 7.55−7.34 (m, 3 H), 7.07 (s, 1 H), 5.41 (s, 1 H), 3.10 (s, 3 H), 2.85 (s, 3 H), 1.27 (s, 9 H). MS ($C_{20}H_{23}N_3O_3$): m/z 354 (M + H)$^+$.

2-(*tert*-Butoxy)-2-(5-methyl-2-phenyl-7-(*p*-tolylamino)-pyrazolo[1,5-*a*]pyrimidin-6-yl)acetic Acid (17). The title compound was prepared from methyl 2-*tert*-butoxy-2-(7-chloro-5-methyl-2-phenylpyrazolo[1,5-*a*]pyrimidin-6-yl)acetate in a manner similar to that described for **19**. ^{1}H NMR (500 MHz, DMSO-d_6) δ (ppm): 7.84−7.83 (m, 2 H), 7.43−7.35 (m, 4H), 7.10 (d, J = 7.9 Hz, 2H), 6.92 (s, 1H), 6.87 (br s, 1H), 5.29 (s, 1H), 2.54 (s, 3H), 2.30 (s, 3H), 1.08 (s, 9H). MS ($C_{26}H_{28}N_4O_3$): m/z 445 (M + H)$^+$.

2-(7-(Azepan-1-yl)-5-methyl-2-phenylpyrazolo[1,5-*a*]-pyrimidin-6-yl)-2-(*tert*-butoxy)acetic Acid (18). The title compound was prepared from methyl 2-*tert*-butoxy-2-(7-chloro-5-methyl-2-phenylpyrazolo[1,5-*a*]pyrimidin-6-yl)acetate in a manner similar to that described for **19**. ^{1}H NMR (500 MHz, DMSO-d_6) δ (ppm): 8.06 (d, J = 7.5 Hz, 2H), 7.54−7.48 (m, 2 H), 7.45−7.41 (m, 1 H), 7.06 (s, 1 H), 5.88 (s, 1 H), 2.55 (s, 3 H), 1.92−1.79 (m, 8 H), 1.22 (s, 9 H). MS ($C_{25}H_{32}N_4O_3$): m/z 437 (M + H)$^+$.

2-(*tert*-Butoxy)-2-(7-(4,4-dimethylpiperidin-1-yl)-5-methyl-2-phenylpyrazolo[1,5-*a*]pyrimidin-6-yl)acetic Acid (19). DIEA (0.047 mL, 0.272 mmol) was added to a mixture of **41** (40 mg, 0.091 mmol) and 4,4-dimethylpiperidine, HCl salt (13.55 mg, 0.091 mmol) in NMP (1 mL) and heated at 50°C for 2 h. 1 N LiOH (0.272 mL, 0.272 mmol) was added to the reaction mixture, and the contents were heated at 50°C for 2 h. The reaction mixture was filtered and the filtrate purified by preparative HPLC to afford **19** as TFA salt (13.5

https://dx.doi.org/10.1021/acs.jmedchem.9b01681
J. Med. Chem. XXXX, XXX, XXX−XXX

mg, 30%). ^{1}H NMR (500 MHz, DMSO-d_6) δ (ppm): 8.05 (d, J = 7.8 Hz, 2H). 7.54−7.48 (m, 2 H), 7.45−7.41 (m, 1 H), 7.03 (s, 1 H), 5.77 (s, 1 H), 2.53 (s, 3 H), 1.65−1.52 (m, 4 H), 1.20 (s, 9 H), 1.12 (br s, 6H). MS ($C_{26}H_{34}N_4O_3$): m/z 451 (M + H)$^+$.

2-*tert*-Butoxy-2-(7-(8-fluoro-5-methylchroman-6-yl)-5-methyl-2-*p*-tolylpyrazolo[1,5-*a*]pyrimidin-6-yl)acetic Acid, TFA Salt (*S*,*S* and *R*,*R*)-20. A mixture of the TFA salt of **47** (8 mg, 0.016 mmol), $Pd(PPh_3)_4$ (2.69 mg, 2.326 μmol), 2-(8-fluoro-5-methylchroman-6-yl)-4,4,5,5-tetramethyl-1,3,2-dioxaborolane (9.06 mg, 0.031 mmol), 2 M K_3PO_4 solution (50 μL), and DMF (0.7 mL) was heated in a microwave reactor at 130 °C for 15 min. The reaction mixture was filtered and the filtrate purified by preparative HPLC to afford methyl 2-*tert*-butoxy-2-(7-(8-fluoro-5-methylchroman-6-yl)-5-methyl-2-*p*-tolylpyrazolo[1,5-*a*]pyrimidin-6-yl)acetate as the TFA salt (5 mg, 49.9%). ^{1}H NMR (400 MHz, $CDCl_3$) δ (ppm): 7.72 (d, J = 8.0 Hz, 2H), 7.21 (d, J = 8.0 Hz, 2H), 7.01 (s, 1 H), 6.89 (d, J = 10.5 Hz, 1H), 5.06 (s, 1 H), 4.40−4.33 (m, 2 H), 3.68 (s, 3 H), 2.86 (s, 3 H), 2.81−2.76 (m, 2 H), 2.38 (s, 3 H), 2.23−2.16 (m, 2 H), 1.86 (s, 3 H), 1.19 (s, 9 H). MS ($C_{31}H_{34}FN_3O_4$): m/z 532 (M + H)$^+$. A mixture of 1 N LiOH aqueous solution (0.5 mL, 0.5 mmol) and methyl 2-*tert*-butoxy-2-(7-(8-fluoro-5-methylchroman-6-yl)-5-methyl-2-*p*-tolylpyrazolo[1,5-*a*]pyrimidin-6-yl)acetate, TFA salt (5 mg, 7.74 μmol) in dioxane (0.5 mL) was stirred at 50 °C for 1 h. The mixture was filtered and the filtrate purified by preparative HPLC to afford (*S*,*S* and *R*,*R*)-**20** (4 mg, 82%) as the TFA salt. ^{1}H NMR (500 MHz, MeOD) δ (ppm): 7.71 (d, J = 8.2 Hz, 2H), 7.21 (d, J = 7.9 Hz, 2H), 6.94 (d, J = 10.7 Hz, 1H), 6.88 (s, 1 H), 5.01 (s, 1 H), 4.40−4.24 (m, 2 H), 2.86−2.78 (m, 2 H), 2.76 (s, 3 H), 2.35 (s, 3 H), 2.22−2.10 (m, 2 H), 1.87 (s, 3 H), 1.17 (s, 9 H). MS ($C_{30}H_{32}FN_3O_4$): m/z 518 (M + H)$^+$.

2-(2-(4-(Benzyloxy)phenyl)-7-(8-fluoro-5-methylchroman-6-yl)-5-methylpyrazolo[1,5-*a*]pyrimidin-6-yl)-2-*tert*-butoxyacetic Acid, TFA Salt ((*S*,*S* and *R*,*R*)-21). The title compound was prepared from methyl 2-(2-bromo-7-chloro-5-methylpyrazolo[1,5-*a*]pyrimidin-6-yl)-2-*tert*-butoxyacetate in a manner similar to that described for compound (*S*,*S* and *R*,*R*)-**20**. ^{1}H NMR (400 MHz, $CDCl_3$) δ (ppm): 7.76 (d, J = 8.8 Hz, 2H), 7.47−7.32 (m, 5H), 7.04−6.95 (m, 3H), 6.91 (d, J = 10.5 Hz, 1H), 5.11 (d, J = 2.0 Hz, 3H), 4.44−4.25 (m, 2H), 2.92−2.59 (m, 5H), 2.28−2.10 (m, 2H), 1.89 (s, 3H), 1.22 (s, 9H). MS ($C_{36}H_{36}FN_3O_5$): m/z 610 (M + H)$^+$.

2-(2-(3-(Benzyloxy)phenyl)-7-(8-fluoro-5-methylchroman-6-yl)-5-methylpyrazolo[1,5-*a*]pyrimidin-6-yl)-2-*tert*-butoxyacetic Acid, TFA Salt ((*S*,*S* and *R*,*R*)-22). The title compound was prepared from methyl 2-(2-bromo-7-chloro-5-methylpyrazolo[1,5-*a*]pyrimidin-6-yl)-2-*tert*-butoxyacetate in a manner similar to that described for compound (*S*,*S* and *R*,*R*)-**20**. ^{1}H NMR (500 MHz, $CDCl_3$) δ (ppm): 7.48−7.27 (m, 8H), 6.96 (dd, J = 8.2, 1.8 Hz, 1H), 6.93−6.88 (m, 2H), 5.08 (s, 3H), 4.46−4.12 (m, 2H), 2.92−2.73 (m, 5H), 2.26−2.08 (m, 2H), 1.91 (s, 3H), 1.20 (s, 9H). MS ($C_{36}H_{36}FN_3O_5$): m/z 610 (M + H)$^+$.

2-*tert*-Butoxy-2-(7-(8-fluoro-5-methylchroman-6-yl)-5-methyl-2-(3-phenoxyphenyl)pyrazolo[1,5-*a*]pyrimidin-6-yl)-acetic Acid, TFA Salt ((*S*,*S* and *R*,*R*)-23). The title compound was prepared from methyl 2-(2-bromo-7-chloro-5-methylpyrazolo[1,5-*a*]pyrimidin-6-yl)-2-*tert*-butoxyacetate in a manner similar to that described for (*S*,*S* and *R*,*R*)-**20**. ^{1}H NMR (400 MHz, $CDCl_3$) δ (ppm): 7.62−7.49 (m, 2H), 7.41−7.31 (m, 3H), 7.17−6.95 (m, 5H), 6.90 (d, J = 10.8 Hz, 1H), 5.12 (s, 1H), 4.50−4.22 (m, 2H), 2.89−2.66 (m, 5H), 2.17 (dd, J = 6.0, 4.0 Hz, 2H), 1.90 (s, 3H), 1.28−1.09 (m, 9H). MS ($C_{35}H_{34}FN_3O_5$): m/z 596 (M + H)$^+$.

2-(2-([1,1′-Biphenyl]-3-yl)-7-(8-fluoro-5-methylchroman-6-yl)-5-methylpyrazolo[1,5-*a*]pyrimidin-6-yl)-2-(*tert*-butoxy)-acetic Acid, TFA Salt ((*S*,*S* and *R*,*R*)-24). The title compound was prepared from methyl 2-(2-bromo-7-chloro-5-methylpyrazolo[1,5-*a*]pyrimidin-6-yl)-2-*tert*-butoxyacetate in a manner similar to that described for (*S*,*S* and *R*,*R*)-**20**. ^{1}H NMR (500 MHz, $CDCl_3$) δ (ppm): 8.05−7.98 (m, 1H), 7.81 (d, J = 7.6 Hz, 1H), 7.65−7.58 (m, 2H), 7.55 (d, J = 7.6 Hz, 1H), 7.46 (t, J = 7.5 Hz, 3H), 7.40−7.33 (m, 1H), 6.98−6.90 (m, 2H), 5.09 (s, 1H), 4.38−4.27 (m, 2H), 2.82−2.66 (m, 5H), 2.15 (d, J = 6.1 Hz, 2H), 1.93 (s, 3H), 1.21 (s, 9H). MS ($C_{35}H_{34}FN_3O_4$): m/z 580 (M + H)$^+$.

(2*S*)-2-(2-([1,1′-Biphenyl]-3-yl)-7-(8-fluoro-5-methylchroman-6-yl)-5-methylpyrazolo[1,5-*a*]pyrimidin-6-yl)-2-(*tert*-butoxy)acetic Acid ((*S*,*S*)-24). The title compound was prepared from (2*S*)-methyl 2-(*tert*-butoxy)-2-(2-(3-chlorophenyl)-7-(8-fluoro-5-methylchroman-6-yl)-5-methylpyrazolo[1,5-*a*]pyrimidin-6-yl)-acetate in a manner similar to that described for (*S*,*S*)-**27**. ^{1}H NMR (500 MHz, $CDCl_3$) δ (ppm): 8.05−7.98 (m, 1H), 7.81 (d, J = 7.6 Hz, 1H), 7.65−7.58 (m, 2H), 7.55 (d, J = 7.6 Hz, 1H), 7.46 (t, J = 7.5 Hz, 3H), 7.40−7.33 (m, 1H), 6.98−6.90 (m, 2H), 5.09 (s, 1H), 4.38−4.27 (m, 2H), 2.82−2.66 (m, 5H), 2.15 (d, J = 6.1 Hz, 2H), 1.93 (s, 3H), 1.21 (s, 9H). MS ($C_{35}H_{34}FN_3O_4$): m/z 580 (M + H)$^+$.

2-(2-([1,1′-Biphenyl]-3-yl)-7-(4,4-dimethylpiperidin-1-yl)-5-methylpyrazolo[1,5-*a*]pyrimidin-6-yl)-2-(*tert*-butoxy)acetic Acid ((*S* and *R*)-25). A mixture of **46** (90 mg, 0.230 mmol), $Pd(PPh_3)_4$ (40 mg, 0.035 mmol), [1,1′-biphenyl]-3-ylboronic acid (45.6 mg, 0.230 mmol), 2 M K_2CO_3 solution (300 μL), and DMF (4 mL) was heated in a microwave reactor at 70 °C for 60 min. The mixture was filtered and the filtrate purified by preparative HPLC to afford methyl 2-(2-([1,1′-biphenyl]-3-yl)-7-chloro-5-methylpyrazolo-[1,5-*a*]pyrimidin-6-yl)-2-(*tert*-butoxy)acetate as the TFA salt (47 mg, 35.3%). MS ($C_{26}H_{26}ClN_3O_3$): m/z 464 (M + H)$^+$. A mixture of methyl 2-(2-([1,1′-biphenyl]-3-yl)-7-chloro-5-methylpyrazolo[1,5-*a*]-pyrimidin-6-yl)-2-(*tert*-butoxy)acetate, TFA salt (25 mg, 0.043 mmol), 4,4-dimethylpiperidine HCl salt (16.13 mg, 0.108 mmol), and DIEA (0.038 mL, 0.216 mmol) in CH_2Cl_2 (3 mL) was stirred at rt for 18 h. The solvent was evaporated, dioxane (1 mL) and NaOH (1 mL, 1.0 mmol) added and the mixture heated at 50 °C for 1 h. The mixture was filtered and the filtrate was purified by preparative HPLC to afford (*S* and *R*)-**25** as the TFA salt (1.5 mg, 6.7%). ^{1}H NMR (500 MHz, DMSO-d_6) δ (ppm): 8.36 (s, 1H), 8.04 (d, J = 7.6 Hz, 1H), 7.79−7.71 (m, 3H), 7.61 (t, J = 7.63 Hz, 1H), 7.52 (t, J = 7.27 Hz, 2H), 7.44−7.41 (m, 1H), 7.11 (s, 1H), 5.63 (br s, 1H), 3.48−3.26 (m, 4H), 2.54 (s, 3H), 1.67−1.51 (m, 4H), 1.18 (s, 9H), 1.12 (br s, 6H). MS ($C_{32}H_{38}N_4O_3$): m/z 527 (M + H)$^+$.

2-(2-(3-(Benzyloxy)phenyl)-7-(4,4-dimethylpiperidin-1-yl)-5-methylpyrazolo[1,5-*a*]pyrimidin-6-yl)-2-(*tert*-butoxy)acetic Acid ((*S* and *R*)-26). The title compound was prepared from methyl 2-(2-bromo-7-chloro-5-methylpyrazolo[1,5-*a*]pyrimidin-6-yl)-2-*tert*-butoxyacetate in a manner similar to that described for (*S* and *R*)-**25**. ^{1}H NMR (500 MHz, DMSO-d_6) δ (ppm): 7.72−7.67 (m, 1H), 7.63 (d, J = 7.6 Hz, 1H), 7.51 (d, J = 7.2 Hz, 2H), 7.44−7.41 (m, 3H), 7.37−7.34 (m, 1H), 7.07 (dd, J = 8.2, 1.8 Hz, 1H), 7.03 (s, 1H), 5.71 (s, 1H), 5.21 (s, 2H), 3.36 (br s, 4H), 2.52 (s, 3H), 1.51−1.67 (m, 4H), 1.19 (s, 9H), 1.11 (br s, 6H). MS ($C_{33}H_{40}N_4O_4$): m/z 557 (M + H)$^+$.

(2*S*)-2-(*tert*-Butoxy)-2-(7-(8-fluoro-5-methylchroman-6-yl)-5-methyl-2-(2′-methyl-[1,1′-biphenyl]-3-yl)pyrazolo[1,5-*a*]-pyrimidin-6-yl)acetic Acid ((*S*,*S*)-27). A mixture of dicyclohexyl-(2′,6′-dimethoxy-[1,1′-biphenyl]-2-yl)phosphine (595 mg, 1.449 mmol), $Pd(OAc)_2$ (163 mg, 0.725 mmol), *o*-tolylboronic acid (296 mg, 2.174 mmol), 2 M K_3PO_4 solution (200 μL), and **55** (400 mg, 0.725 mmol) in DMF (1.5 mL) was heated in a microwave reactor at 130 °C for 30 min. The mixture was filtered and the filtrate purified by silica gel chromatography to afford (2*S*)-methyl 2-(*tert*-butoxy)-2-(7-(8-fluoro-5-methylchroman-6-yl)-5-methyl-2-(2′-methyl-[1,1′-biphenyl]-3-yl)pyrazolo[1,5-*a*]pyrimidin-6-yl)acetate (225.6 mg, 51.2%). ^{1}H NMR (500 MHz, $CDCl_3$) δ (ppm): 7.86−7.76 (m, 2H), 7.42 (t, J = 7.8 Hz, 1H), 7.29−7.26 (m, 5H), 6.88−6.86 (m, 2H), 4.99 (s, 1H), 4.39−4.27 (m, 2H), 3.64 (s, 3H), 2.83−2.70 (m, 5H), 2.26 (s, 3H), 2.22−2.13 (m, 2H), 1.84 (s, 3H), 1.16 (s, 9H). MS ($C_{37}H_{38}FN_3O_4$): m/z 608 (M + H)$^+$. 1 N NaOH aqueous solution (9 mL, 9 mmol) was added to a solution of (2*S*)-methyl 2-(*tert*-butoxy)-2-(7-(8-fluoro-5-methylchroman-6-yl)-5-methyl-2-(2′-methyl-[1,1′-biphenyl]-3-yl)pyrazolo[1,5-*a*]pyrimidin-6-yl)acetate (1.28 g, 2.1 mmol) in dioxane (12 mL) and the mixture stirred at 50 °C for 2 h. The mixture was diluted with H_2O (50 mL), neutralized with AcOH, and extracted with EtOAc (3 × 100 mL). The organic phase was combined, dried over Na_2SO_4, concentrated and the crude product purified by preparative HPLC to afford (*S*,*S*)-**27** (840 mg, 66%). ^{1}H NMR (400 MHz, DMSO-d_6) δ (ppm): 7.86−7.75 (m, 2H), 7.50 (t, J = 7.7 Hz, 1H), 7.40−7.22 (m, 5H), 7.18 (s, 1H), 7.09 (d, J =

https://dx.doi.org/10.1021/acs.jmedchem.9b01681
J. Med. Chem. XXXX, XXX, XXX−XXX

1.0 Hz, 1H), 4.83 (s, 1H), 4.34−4.22 (m, 2H), 2.82−2.66 (m, 5H), 2.24 (s, 3H), 2.13−2.02 (m, 2H), 1.83 (s, 3H), 1.09 (s, 9H). MS ($C_{36}H_{36}FN_3O_4$): m/z 594 $(M + H)^+$. Anal. ($C_{36}H_{36}FN_3O_4$ with 1.26% H_2O) Calcd: C, 71.91; H, 6.18; N, 6.99; F, 3.16. Found: C, 71.67; H, 6.25; N, 7.07; F, 2.79.

(2*S*)-2-(*tert*-Butoxy)-2-(7-(8-fluoro-5-methylchroman-6-yl)-2-(2′-methoxy-[1,1′-biphenyl]-3-yl)-5-methylpyrazolo[1,5-*a*]pyrimidin-6-yl)acetic Acid ((*S*,*S*)-28). The title compound was prepared from (2*S*)-methyl 2-(*tert*-butoxy)-2-(2-(3-chlorophenyl)-7-(8-fluoro-5-methylchroman-6-yl)-5-methylpyrazolo[1,5-*a*]pyrimidin-6-yl)acetate in a manner similar to that described for (*S*,*S*)-**27**. ^1H NMR (500 MHz, $CDCl_3$) δ (ppm): 8.00−7.95 (m, 1H), 7.79 (d, J = 7.6 Hz, 1H), 7.51−7.47 (m, 1H), 7.45−7.39 (m, 1H), 7.37−7.31 (m, 2H), 7.08−6.97 (m, 2H), 6.93 (d, J = 10.7 Hz, 1H), 6.90 (s, 1H), 5.08 (s, 1H), 4.39−4.24 (m, 2H), 3.79 (s, 3H), 2.82−2.64 (m, 5H), 2.15 (d, J = 3.7 Hz, 2H), 1.92 (s, 3H), 1.21 (s, 9H). MS ($C_{36}H_{36}FN_3O_5$): m/z 610 $(M + H)^+$.

(2*S*)-2-(*tert*-Butoxy)-2-(7-(8-fluoro-5-methylchroman-6-yl)-2-(2′-fluoro-[1,1′-biphenyl]-3-yl)-5-methylpyrazolo[1,5-*a*]pyrimidin-6-yl)acetic Acid ((*S*,*S*)-29). The title compound was prepared from (2*S*)-methyl 2-(*tert*-butoxy)-2-(2-(3-chlorophenyl)-7-(8-fluoro-5-methylchroman-6-yl)-5-methylpyrazolo[1,5-*a*]pyrimidin-6-yl)acetate in a manner similar to that described for (*S*,*S*)-**27**. ^1H NMR (500 MHz, $CDCl_3$) δ (ppm): 7.95 (d, J = 1.2 Hz, 1H), 7.88−7.75 (m, 1H), 7.57−7.40 (m, 3H), 7.37−7.29 (m, 1H), 7.24−7.12 (m, 2H), 7.01−6.82 (m, 2H), 5.06 (s, 1H), 4.36−4.24 (m, 2H), 2.80−2.63 (m, 5H), 2.13 (dd, J = 6.1, 3.1 Hz, 2H), 1.89 (s, 3H), 1.17 (s, 9H). MS ($C_{35}H_{33}F_2N_3O_4$): m/z 598 $(M + H)^+$.

(2*S*)-2-(*tert*-Butoxy)-2-(7-(8-fluoro-5-methylchroman-6-yl)-5-methyl-2-(3-(pyridin-4-yl)phenyl)pyrazolo[1,5-*a*]pyrimidin-6-yl)acetic Acid, TFA Salt ((*S*,*S*)-30). The title compound was prepared from (2*S*)-methyl 2-(*tert*-butoxy)-2-(2-(3-chlorophenyl)-7-(8-fluoro-5-methylchroman-6-yl)-5-methylpyrazolo[1,5-*a*]pyrimidin-6-yl)acetate in a manner similar to that described for (*S*,*S*)-**27**. ^1H NMR (500 MHz, $CDCl_3$) δ (ppm): 8.91 (d, J = 6.41 Hz, 2H), 8.13−8.05 (m, 4H), 7.75−7.60 (m, 2H), 7.00 (s, 1H), 6.92 (d, J = 10.38 Hz, 1H), 5.09 (s, 1H), 4.33 (t, J = 5.04 Hz, 2H), 2.79−2.69 (m, 5H), 2.22−2.11 (m, 2H), 1.95 (s, 3H), 1.21 (s, 9H). MS ($C_{34}H_{33}FN_4O_4$): m/z 581 $(M + H)^+$. HRMS calcd for $C_{34}H_{33}FN_4O_4$ (MH^+) 581.2559, found 581.2574.

(2*S*)-2-(*tert*-Butoxy)-2-(7-(8-fluoro-5-methylchroman-6-yl)-2-(3-(6-methoxypyridin-3-yl)phenyl)-5-methylpyrazolo[1,5-*a*]pyrimidin-6-yl)acetic Acid ((*S*,*S*)-31). The title compound was prepared from (2*S*)-methyl 2-(*tert*-butoxy)-2-(2-(3-chlorophenyl)-7-(8-fluoro-5-methylchroman-6-yl)-5-methylpyrazolo[1,5-*a*]pyrimidin-6-yl)acetate in a manner similar to that described for (*S*,*S*)-**27**. ^1H NMR (500 MHz, DMSO-d_6) δ (ppm): 8.55 (d, J = 2.4 Hz, 1H), 8.13−8.05 (m, 2H), 7.79 (d, J = 7.9 Hz, 1H), 7.66 (d, J = 7.9 Hz, 1H), 7.51 (t, J = 7.6 Hz, 1H), 7.26 (s, 1H), 7.09 (d, J = 11.3 Hz, 1H), 6.95 (d, J = 8.5 Hz, 1H), 4.78 (s, 1H), 4.34−4.21 (m, 2H), 3.92 (s, 3H), 2.75−2.73 (m, 2H), 2.71 (s, 3H), 2.08 (t, J = 5.6 Hz, 2H), 1.83 (s, 3H), 1.09 (s, 9H). MS ($C_{35}H_{35}FN_4O_5$): m/z 611 $(M + H)^+$.

Methyl 5-Methyl-2-phenyl-7-*p*-tolylpyrazolo[1,5-*a*]pyrimidine-6-carboxylate (34). To a stirred solution of 4-methylbenzaldehyde **32** (1.2 g, 9.99 mmol), 3-phenyl-1*H*-pyrazol-5-amine **33** (1.6 g, 9.99 mmol), and methyl 3-oxobutanoate (1.3 g, 10.99 mmol) in THF (80 mL) and heptane (20 mL) was added piperidine (30 μL, 0.303 mmol). The reaction mixture was heated at reflux for 20 h, the solvent was evaporated, and the crude material was dissolved in CH_2Cl_2. DDQ (2.041 g, 8.99 mmol) was added, and the mixture was stirred at room temperature for 1 h. The solvent was evaporated and the residue purified by silica gel chromatography to provide **34** (2.3 g, 64%). ^1H NMR (500 MHz, $CDCl_3$) δ (ppm): 7.99−7.86 (m, 2H), 7.63 (d, J = 7.9 Hz, 2H), 7.47−7.31 (m, 5H), 6.93 (s, 1 H), 3.64 (s, 3 H), 2.65 (s, 3 H), 2.47 (s, 3 H). MS ($C_{22}H_{19}N_3O_2$): m/z 358 $(M + H)^+$.

5-Methyl-2-phenyl-7-*p*-tolylpyrazolo[1,5-*a*]pyrimidine-6-carbaldehyde (35). DIBAL-H (1 M in THF, 6.72 mL, 6.72 mmol) was added dropwise to a stirred solution of **34** (800 mg, 2.238 mmol) in CH_2Cl_2 (50 mL). The reaction mixture was stirred at room temperature for 1 h before being quenched with saturated NH_4Cl solution. The aqueous layer was extracted with CH_2Cl_2, and the combined organic layer was dried over anhydrous Na_2SO_4, filtered, and concentrated. The residue was purified by silica gel chromatography to give (5-methyl-2-phenyl-7-*p*-tolylpyrazolo[1,5-*a*]pyrimidin-6-yl)methanol (344 mg, 46.7%). ^1H NMR (500 MHz, $CDCl_3$) δ (ppm): 1.61 (1 H, t, J = 5.0 Hz), 2.49 (3 H, s), 2.78 (3 H, s), 4.59 (2 H, d, J = 5.0 Hz), 6.88 (1 H, s), 7.29−7.42 (5 H, m), 7.56 (2 H, d, J = 8.2 Hz), 7.81−7.96 (2 H, m). MS ($C_{21}H_{19}N_3O$): m/z 330 $(M + H)^+$.

To a stirred solution of (5-methyl-2-phenyl-7-*p*-tolylpyrazolo[1,5-*a*]pyrimidin-6-yl)methanol (100 mg, 0.304 mmol) in CH_2Cl_2 (8 mL) was added PCC (98 mg, 0.455 mmol). The reaction mixture was stirred at room temperature for 16 h. The solvent was evaporated and the residue was purified by silica gel chromatography to give the title compound **35** (82 mg, 83%). ^1H NMR (500 MHz, $CDCl_3$) δ (ppm): 9.80 (s, 1 H), 7.91 (dd, J = 8.1, 1.4 Hz, 2H), 7.60 (d, J = 7.9 Hz, 2H), 7.50−7.33 (m, 5 H), 6.98 (s, 1 H), 2.89 (s, 3 H), 2.52 (s, 3 H). MS ($C_{21}H_{17}N_3O$): m/z 328 $(M + H)^+$.

2-Hydroxy-2-(5-methyl-2-phenyl-7-*p*-tolylpyrazolo[1,5-*a*]pyrimidin-6-yl)acetonitrile (36). To a solution of **35** (30 mg, 0.092 mmol) in CH_2Cl_2 (2 mL) at 0 °C was added ZnI_2 (14.63 mg, 0.046 mmol) followed by TMS-CN (0.049 mL, 0.367 mmol). The reaction mixture was stirred at room temperature for 4 h and diluted with CH_2Cl_2 (100 mL), washed with H_2O, and dried over Na_2SO_4. The solvent was evaporated and the residue was purified by preparative HPLC to give the title compound **36** (15 mg, 46.2%) as a TFA salt. ^1H NMR (500 MHz, $CDCl_3$) δ (ppm): 7.76−7.63 (m, 2 H), 7.44−7.30 (m, 4 H), 7.25−7.16 (m, 3 H), 6.85 (s, 1 H), 5.39 (s, 1 H), 2.89 (s, 3 H), 2.46 (s, 3 H). MS ($C_{22}H_{18}N_4O$): m/z 355 $(M + H)^+$.

Methyl 2-(5-Methyl-7-oxo-2-phenyl-4,7-dihydropyrazolo-[1,5-*a*]pyrimidin-6-yl)acetate (38). *p*-TsOH.H_2O (50 mg, 0.263 mmol) was added to a solution of 3-phenyl-1*H*-pyrazol-5-amine **33** (4 g, 25.1 mmol) and dimethyl 2-acetylsuccinate **37** (12 mL, 74.0 mmol) in xylene (120 mL) and the mixture heated at reflux under a Dean−Stark trap for 20 h. The solid was filtered and washed with hexanes to afford **38** (6.4 g, 86%). ^1H NMR (400 MHz, MeOD) δ (ppm): 8.06−7.87 (m, 2 H), 7.53−7.34 (m, 3 H), 6.46 (s, 1 H), 3.72 (s, 3 H), 3.66 (s, 2 H), 2.37 (s, 3 H). MS ($C_{16}H_{15}N_3O_3$): m/z 298 $(M + H)^+$.

Methyl 2-(7-Chloro-5-methyl-2-phenylpyrazolo[1,5-*a*]pyrimidin-6-yl)acetate (39). $POCl_3$ (25 mL, 268 mmol) was added to **38** (3 g, 10.09 mmol) and the mixture heated at reflux for 1 h. After cooling, the reaction mixture was added dropwise to ice−water to afford a brown precipitate. The solid was filtered off, washed with H_2O, and dissolved in EtOAc. The organic solution was washed with saturated $NaHCO_3$ and dried over Na_2SO_4. The solvent was evaporated to give **39** (2.77 g, 84%). ^1H NMR (400 MHz, DMSO-d_6) δ (ppm): 8.07 (d, J = 7.0 Hz, 2H), 7.58−7.43 (m, 3 H), 7.29 (s, 1 H), 4.04 (s, 2 H), 3.71 (s, 3 H), 2.58 (s, 3 H). MS ($C_{16}H_{14}ClN_3O_2$): m/z 316 $(M + H)^+$.

Methyl 2-(7-Chloro-5-methyl-2-phenylpyrazolo[1,5-*a*]pyrimidin-6-yl)-2-hydroxyacetate (40). A solution of **39** (1 g, 3.17 mmol) in THF (24 mL) was added dropwise over 40 min to a stirred solution of KHMDS (0.5 M in toluene, 9.50 mL, 4.75 mmol) in THF (24 mL) maintained at −78 °C. The mixture was stirred at −78 °C for 30 min before adding a solution of 3-phenyl-2-(phenylsulfonyl)-1,2-oxaziridine (1.241 g, 4.75 mmol) in THF (24 mL) over 20 min. The reaction mixture was stirred for additional 30 min at −78 °C before being quenched by the addition of saturated aqueous NH_4Cl solution (4 mL). The reaction mixture was allowed to warm to room temperature, diluted with EtOAc (100 mL) and the organic phase washed with H_2O and brine and dried over Na_2SO_4. The solvent was evaporated and the residue purified by silica gel chromatography to provide **40** (535 mg, 50.9%). ^1H NMR (500 MHz, $CDCl_3$) δ ppm: 8.02−8.00 (m, 2 H), 7.50−7.38 (m, 3 H), 6.94 (s, 1 H), 5.76 (s, 1 H), 5.29 (s, 1 H), 3.83 (s, 3 H), 2.62 (s, 3 H). MS ($C_{16}H_{14}ClN_3O_3$): m/z 332 $(M + H)^+$.

Methyl 2-*tert*-Butoxy-2-(7-chloro-5-methyl-2-phenylpyrazolo[1,5-*a*]pyrimidin-6-yl)acetate (41). CH_2Cl_2 (2 mL) and $HClO_4$ (0.027 mL, 0.452 mmol) were added sequentially to a suspension of methyl 2-(7-chloro-5-methyl-2-phenylpyrazolo[1,5-*a*]pyrimidin-6-yl)-2-hydroxyacetate **40** (100 mg, 0.301 mmol) in *tert*-

https://dx.doi.org/10.1021/acs.jmedchem.9b01681
J. Med. Chem. XXXX, XXX, XXX−XXX

butyl acetate (2 mL), and the mixture was stirred for 2 h at room temperature. The reaction mixture was quenched with H_2O, diluted with EtOAc and the organic phase washed with saturated $NaHCO_3$ and dried over Na_2SO_4. The solvent was evaporated and the residue purified by silica gel chromatography to provide **41** (71 mg, 60.7%). ^{1}H NMR (500 MHz, $CDCl_3$) δ (ppm): 8.01 (d, J = 7.3 Hz, 2H), 7.52−7.34 (m, 3 H), 6.93 (s, 1 H), 5.66 (s, 1 H), 3.73 (s, 3 H), 1.27 (s, 9 H). MS ($C_{20}H_{22}ClN_3O_3$): m/z 388 $(M + H)^+$.

Methyl 2-(2-Bromo-7-hydroxy-5-methylpyrazolo[1,5-*a*]pyrimidin-6-yl)acetate (43). *p*-TsOH·H_2O (2 mg, 10.51 μmol) was added to a solution of **42** (0.2 g, 1.235 mmol) and **37** (0.697 g, 3.70 mmol) in xylene (10 mL) and the mixture heated at reflux under a Dean−Stark trap for 8 h. The solid was filtered and washed with hexanes to afford **43** (0.201 g, 54.2%). ^{1}H NMR (400 MHz, MeOD) δ (ppm): 6.20 (s, 1 H), 3.71 (s, 3 H), 3.65 (s, 2 H), 2.37 (s, 3 H). MS ($C_{10}H_{10}BrN_3O_3$): m/z 300 $(M + H)^+$.

Methyl 2-(2-Bromo-7-chloro-5-methylpyrazolo[1,5-*a*]pyrimidin-6-yl)acetate (44). $POCl_3$ (1 mL, 10.73 mmol) was added to **43** (180 mg, 0.600 mmol) and the mixture heated at reflux for 1 h. After cooling, the reaction mixture was added dropwise to ice−water to afford a brown solid precipitate. The solid was filtered off and washed with H_2O to give **44** (158 mg, 83%). ^{1}H NMR (500 MHz, DMSO-d_6) δ (ppm): 6.99 (s, 1 H), 4.01 (s, 2 H), 3.69 (s, 3 H), 2.56 (s, 3 H). MS ($C_{10}H_9BrClN_3O_2$): m/z 318 $(M + H)^+$.

Methyl 2-(2-Bromo-7-chloro-5-methylpyrazolo[1,5-*a*]pyrimidin-6-yl)-2-hydroxyacetate (45). A solution of **44** (300 mg, 0.942 mmol) in THF (6 mL) was added dropwise over 20 min to a stirred solution of KHMDS (0.5 M in toluene, 2.83 mL, 1.413 mmol) in THF (6 mL) maintained at −78 °C. The mixture was stirred at −78 °C for 30 min before adding a solution of 3-phenyl-2-(phenylsulfonyl)-1,2-oxaziridine (369 mg, 1.413 mmol) in THF (6 mL) over 15 min. The mixture was stirred for an additional 60 min at −78 °C before being quenched with saturated NH_4Cl aqueous solution (4 mL). The mixture was allowed to warm to room temperature, diluted with EtOAc (100 mL) and the organic phase washed with H_2O and brine before being dried over Na_2SO_4. The solvent was evaporated and the residue purified by silica gel chromatography to provide **45** (85 mg, 27%). ^{1}H NMR (400 MHz, $CDCl_3$) δ (ppm): 6.71 (s, 1 H), 5.74 (s, 1 H), 3.84 (s, 3 H), 2.63 (s, 3 H). MS ($C_{10}H_9BrClN_3O_3$): m/z 334.

Methyl 2-(2-Bromo-7-chloro-5-methylpyrazolo[1,5-*a*]pyrimidin-6-yl)-2-*tert*-butoxyacetate (46). CH_2Cl_2 (2 mL) and $HClO_4$ (0.022 mL, 0.359 mmol) were added to a suspension of **45** (80 mg, 0.239 mmol) in *tert*-butyl acetate (2 mL) and the mixture stirred for 4 h at room temperature. The reaction mixture was quenched with H_2O, diluted with EtOAc and the organic phase washed with saturated $NaHCO_3$ and dried over Na_2SO_4. The solvent was evaporated and the residue purified by silica gel chromatography to provide **46** (56 mg, 59.9%). ^{1}H NMR (500 MHz, MeOD) δ (ppm): 6.75 (s, 1 H), 5.75 (s, 1 H), 3.74 (s, 3 H), 2.62 (s, 3 H), 1.27 (s, 9 H). MS ($C_{14}H_{17}BrClN_3O_3$): m/z 390.

Methyl 2-*tert*-Butoxy-2-(7-chloro-5-methyl-2-*p*-tolylpyrazolo[1,5-*a*]pyrimidin-6-yl)acetate, TFA Salt (47). A mixture of **46** (28 mg, 0.072 mmol), $Pd(PPh_3)_4$ (12.42 mg, 10.75 μmol), *p*-tolylboronic acid (10.72 mg, 0.079 mmol), 2 M K_2CO_3 solution (100 μL), and DMF (3 mL), was heated in a microwave reactor at 70 °C for 60 min. The mixture was filtered and the filtrate purified by preparative HPLC to afford **47** (16 mg, 43.3%) as the TFA salt. ^{1}H NMR (500 MHz, MeOD) δ (ppm): 7.92 (d, J = 7.9 Hz, 2H), 7.30 (d, J = 7.9 Hz, 2H), 6.98 (s, 1 H), 5.79 (s, 1 H), 3.75 (s, 3 H), 2.62 (s, 3 H), 2.40 (s, 3 H), 1.29 (s, 9 H). MS ($C_{21}H_{24}ClN_3O_3$): m/z 402 $(M + H)^+$.

Methyl 2-(2-(3-Chlorophenyl)-7-hydroxy-5-methylpyrazolo[1,5-*a*]pyrimidin-6-yl)acetate (49). *p*-TsOH·H_2O (100 mg, 0.526 mmol) was added to a solution of **48** (23 g, 119 mmol) and dimethyl 2-acetylsuccinate **37** (22.35 g, 119 mmol) in *o*-xylene (200 mL) and the mixture heated at reflux under a Dean−Stark trap for 2 h. The solid was filtered and washed with hexanes to afford **49** (39 g, 99%). ^{1}H NMR (500 MHz, MeOD) δ (ppm): 8.14−7.95 (m, 1H), 7.93−7.79 (m, 1H), 7.51−7.27 (m, 2H), 6.62−6.35 (m, 1H), 3.72 (s, 3H), 3.67 (s, 2H), 2.39 (s, 3H). MS ($C_{16}H_{14}ClN_3O_3$): m/z 332 $(M + H)^+$.

Methyl 2-(7-Chloro-2-(3-chlorophenyl)-5-methylpyrazolo-[1,5-*a*]pyrimidin-6-yl)acetate (50). A mixture of **49** (12 g, 36.2 mmol) and $POCl_3$ (50 mL) was heated at reflux for 2.5 h. After cooling, the reaction mixture was added dropwise to ice−water to precipitate a brown solid which was filtered and washed with H_2O before dissolving in EtOAc. The organic layer was washed with saturated $NaHCO_3$, dried over Na_2SO_4 and concentrated to give **50** (11.9 g, 94%). ^{1}H NMR (400 MHz, $CDCl_3$) δ (ppm): 8.03 (t, J = 1.8 Hz, 1H), 7.94−7.82 (m, 1H), 7.48−7.34 (m, 2H), 6.94 (s, 1H), 3.93 (s, 2H), 3.78 (s, 3H), 2.63 (s, 3H). MS ($C_{16}H_{13}Cl_2N_3O_2$): m/z 350 $(M + H)^+$.

Methyl 2-(7-Chloro-2-(3-chlorophenyl)-5-methylpyrazolo-[1,5-*a*]pyrimidin-6-yl)-2-hydroxyacetate (51). KHMDS (44.5 mL, 22.27 mmol) was added dropwise over 30 min to a stirred solution of **50** (7.8 g, 22.27 mmol) in THF (40 mL) maintained at −78 °C. The mixture was stirred at −78 °C for 30 min before adding a solution of 3-phenyl-2-(phenylsulfonyl)-1,2-oxaziridine (8.73 g, 33.4 mmol) in THF (50 mL) over 30 min. After stirring for an additional 2 h at −78 °C, the mixture was quenched with saturated NH_4Cl aqueous solution (40 mL) and allowed to warm to room temperature before being diluted with EtOAc (200 mL). The organic phase was washed with H_2O and brine, dried over Na_2SO_4, and concentrated to leave a residue that was purified by silica gel chromatography to provide **51** (4.2 g, 51.5%). ^{1}H NMR (500 MHz, $CDCl_3$) δ (ppm): 8.05−7.97 (m, 1H), 7.88 (dt, J = 6.7, 1.8 Hz, 1H), 7.44−7.38 (m, 2H), 6.93 (s, 1H), 5.76 (s, 1H), 3.84 (s, 3H), 2.62 (s, 3H). MS ($C_{16}H_{13}Cl_2N_3O_3$): m/z 366 $(M + H)^+$.

Methyl 2-(7-Chloro-2-(3-chlorophenyl)-5-methylpyrazolo-[1,5-*a*]pyrimidin-6-yl)-2-oxoacetate (52). Dess−Martin periodinane (6.37 g, 15.02 mmol) was added to a mixture of **51** (5.0 g, 13.65 mmol) in CH_2Cl_2 (20 mL), and the mixture was stirred at room temp for 1 h. The mixture was diluted with EtOAc (100 mL), the organic layer was washed with saturated $NaHCO_3$ solution (100 mL), dried over Na_2SO_4, and concentrated. The residue was purified by silica gel chromatography to afford **52** (3.8 g, 76%). ^{1}H NMR (500 MHz, $CDCl_3$) δ (ppm): 8.10−7.98 (m, 1H), 7.89 (td, J = 4.4, 1.5 Hz, 1H), 7.51−7.36 (m, 2H), 7.00 (s, 1H), 4.00 (s, 3H), 2.62 (s, 3H). MS ($C_{16}H_{11}Cl_2N_3O_3$): m/z 364 $(M + H)^+$.

(*S*)-Methyl 2-(7-Chloro-2-(3-chlorophenyl)-5-methylpyrazolo[1,5-*a*]pyrimidin-6-yl)-2-hydroxyacetate (53). (*R*)-1-Methyl-3,3-diphenylhexahydropyrrolo[1,2-*c*][1,3,2]-oxazaborole/toluene (1.797 mL of a 1.1 M solution, 1.977 mmol) was added to a stirred solution of **52** (1.8 g, 4.94 mmol) in anhydrous toluene (30 mL) and the mixture cooled to −40 °C (acetonitrile/dry ice bath). A solution of catecholborane (50% by weight) in toluene (1.695 mL, 6.92 mmol) was added over 30 min and the mixture stirred at −45 to −35 °C for 2 h and at −25 °C to −15 °C for an additional 1 h. Saturated Na_2CO_3 solution (20 mL) was added to quench the reaction, and the mixture was stirred vigorously for 30 min and extracted with EtOAc. The organic layer was washed with saturated Na_2CO_3 solution, dried over Na_2SO_4, and concentrated to leave a residue that was purified by silica gel chromatography (15−50% EtOAc/hexane) to afford **53** (1.5 g, 83%). ^{1}H NMR (500 MHz, $CDCl_3$) δ (ppm): 8.05−7.97 (m, 1H), 7.88 (dt, J = 6.7, 1.8 Hz, 1H), 7.44−7.38 (m, 2H), 6.93 (s, 1H), 5.76 (s, 1H), 3.84 (s, 3H), 2.62 (s, 3H). MS ($C_{16}H_{13}Cl_2N_3O_3$): m/z 366 $(M + H)^+$.

(*S*)-Methyl 2-(*tert*-Butoxy)-2-(7-chloro-2-(3-chlorophenyl)-5-methylpyrazolo[1,5-*a*]pyrimidin-6-yl)acetate (54). *tert*-Butyl acetate (20 mL) and $HClO_4$ (0.282 mL, 3.28 mmol) were added to a solution of **53** (1.0 g, 2.73 mmol) in CH_2Cl_2 (100 mL), and the mixture was stirred for 16 h at room temperature. The mixture was quenched with H_2O, diluted with EtOAc and the organic phase washed with saturated $NaHCO_3$ and dried over Na_2SO_4. The solvent was evaporated and the residue purified by silica gel chromatography to provide **54** (520 mg, 50%). ^{1}H NMR (400 MHz, $CDCl_3$) δ (ppm): 8.07−8.00 (m, 1H), 7.89 (dt, J = 6.7, 1.9 Hz, 1H), 7.48−7.37 (m, 2H), 6.93 (s, 1H), 5.68 (s, 1H), 3.75 (s, 3H), 2.69 (s, 3H), 1.29 (s, 9H). MS ($C_{20}H_{21}Cl_2N_3O_3$): m/z 422 $(M + H)^+$.

https://dx.doi.org/10.1021/acs.jmedchem.9b01681
J. Med. Chem. XXXX, XXX, XXX−XXX

(2*S*)-Methyl 2-(tert-Butoxy)-2-(2-(3-chlorophenyl)-7-(8-fluoro-5-methylchroman-6-yl)-5-methylpyrazolo[1,5-a]pyrimidin-6-yl)acetate ((*S*,*S*)-55). A mixture of **54** (420 mg, 0.995 mmol), $Pd(PPh_3)_4$ (115 mg, 0.099 mmol), 2-(8-fluoro-5-methylchroman-6-yl)-4,4,5,5-tetramethyl-1,3,2-dioxaborolane (320 mg, 1.094 mmol), 2M K_2CO_3 solution (400 μL) in DMF (4 mL) was heated in a microwave reactor at 125 °C for 45 min. The mixture was filtered and the filtrate purified by silica gel chromatography to afford **55** (204 mg, 37.2%). The enantiomeric excess was determined by a chiral SFC method: Chiralpak AD-H analytical column, 4.6 × 250 mm, 5 m; Mobile Phase: 15% MeOH in CO_2. Temp: 35 °C. Flow rate: 2.0 mL/min. for 10 min. UV monitored @ 266nm. Injection: 5 L of ~2.0 mg/mL solution in 50:50 MeOH:$CHCl_3$. The enantiomeric excess was 93.0%. ^{1}H-NMR (500 MHz, CDCl3) δ (ppm): 7.83−7.78 (m, 1H), 7.69 (dt, *J* = 6.7, 1.8 Hz, 1H), 7.35−7.28 (m, 2H), 6.87 (d, *J* = 10.7 Hz, 1H), 6.84 (s, 1H), 5.00 (s, 1H), 4.48−4.26 (m, 2H), 3.64 (s, 3H), 2.85−2.67 (m, 5H), 2.30−2.13 (m, 2H), 1.84 (s, 3H), 1.16 (s, 9H). MS ($C_{30}H_{31}ClFN_3O_4$): *m*/*z* 552 $(M + H)^+$.

Crystallization, Data Collection, and Structure Refinement for the HIV-1 Integrase CCD:(*S*,*S*)-14 Complex. Crystals of HIV(50-212)-C56S-W131E-F185K were prepared by the sitting drop vapor diffusion method. The protein stock solution consisted of 12.5 mg/mL (0.691 mM based on the calculated MW of 18 098 Da) in 25 mM Hepes, pH 7.5, 500 mM NaCl, 1 mM EDTA, and 5 mM DTT. The addition of 50 mM $MgCl_2$ to the buffer prior to complexing improved crystal screening hits; however, later magnesium was added directly to the crystallization screen. The protein was complexed with 1.74 mM compound **14** from a 100 mM stock solution dissolved in 100% DMSO. The protein/ligand complex was incubated for 4 h at 4 °C and clarified by centrifugation. Crystallization screens were prepared using a SCREENMAKER 96+8 (Innovadyne, Santa Rosa, CA, USA) on MRC 2 well sitting drop trays. Crystals grew from reservoir solution conditions of 2.0 M $(NH_4)_2SO_4$ and 100 mM citric acid, pH 3.5. Drops were formed from 0.8 μL of the protein solution and 0.8 μL of the reservoir solution (total initial volume of 1.6 μL), mixed, and placed at 20 °C to equilibrate. Crystals appeared within 3 days and grew for an additional 7 days. Single crystals were removed and transferred to a cryo-solution consisting of 1.75 M $(NH_4)_2SO_4$, 75 mM citric acid, pH 3.5, 10% (v/v) glycerol, and 10% (v/v) PEG 400. Crystals were flash frozen in liquid N_2 and stored prior to data collection. Data for the HIV-1 integrase/(*S*,*S*)-**14** complex were collected at beamline 17ID at IMCA-CAT of the Advanced Photon Source at Argonne National Laboratory. The wavelength used was 1.0 Å, and the detector was a DECTRIS PILATUS 6M. The diffraction images were indexed, integrated, and scaled with XDS using autoPROC (Global Phasing Ltd., Cambridge, England). The structure was determined by molecular replacement using the program PHASER[26] with a previously reported structure of HIV integrase (PDB entry 6NCJ) used as the starting model in the refinement. The structure was refined with the program autoBUSTER (Global Phasing Ltd., Cambridge, England) and was examined and manually refitted with the program COOT.[27] Grade (Global Phasing Ltd., Cambridge, England) was used to generate a CIF restraint dictionary for (*S*,*S*)-**14**, and rhofit (Global Phasing Ltd., Cambridge, England) was used to place the ligand. Refinement was completed using Coot and autoBUSTER, and the statistics are included in Supporting Information. Display graphics were produced with PyMOL version 1.4 (Schrödinger). The coordinates of the HIV-1 integrase CCD:(*S*,*S*)-**14** complex have been deposited in the PDB under PDB code 6UM8.

Virology Materials and Methods. Competitive Binding Assay Method. Compounds were evaluated for their ability to displace a tritiated LEDGF inhibitor ([^{3}H]-**1**) from binding to HIV-1 integrase via a LEDGF inhibitor displacement assay (LIDIA). Relative inhibitor avidity for HIV-1 integrase is expressed as a K_i value. The final concentrations of reagents in the 50 μL LIDIA assay are 26 mM MOPS buffer, pH 7.0, 11 mM DTT, 100 mM NaCl, 20 mM $MgCl_2$, 0.05% NP-40, 5% PEG-8000, 27 μM [^{3}H]-**1**, 13 μM purified HIV-1 integrase, and 2 mg/mL PVT SPA beads (polyvinyltoluene scintillation proximity assay beads. PerkinElmer, Waltham, MA). Compounds are titrated in 10 μL volumes in 25% DMSO over a final concentration range of 100 μM to 0.0512 nM (ten 5-fold dilutions). Initially, HIV-1 integrase was incubated with PVT SPA beads in 1.25× cocktail (minus [^{3}H]-**1**) for 1 h with rocking in a tube. [^{3}H]-**1** was added, vortexed, and then 40 μL was immediately added to 10 μL of test compound in a white opaque 96-well plate (Corning 3600, Corning, NY). The plate was rocked for 1 h at room temperature in the dark. After sitting in the dark overnight, the plate was read on a Microbeta plate reader (PerkinElmer, Waltham MA). Data were imported into ToolSet (BMS, Wallingford, CT) and analyzed in CurveMaster (BMS, Wallingford, CT) to calculate K_i values.

Cell Lines and Viruses. MT-2 and HEK 293T cells were obtained from the NIH AIDS Research and Reference Reagent Program. Cells were propagated in RPMI 1640 media supplemented with 10% heat inactivated fetal bovine serum, 10 mM HEPES buffer, pH 7.55, 2 mM L-glutamine, 100 units/mL penicillin G, 100 μg/mL streptomycin. The proviral DNA clone of NL_{4-3} was obtained through the NIH AIDS Research and Reference Reagent Program.

For analysis of the potency of ALLINI compounds, an NL_{4-3}-derived replication competent virus, NLRepRluc/SacII (the unique SacII site was engineered at the end of the integrase gene), was generated from a proviral clone. In this clone, a section of the nef gene from NL_{4-3} was replaced with the *Renilla* luciferase gene. This virus is infectious and can undergo multiple cycles of replication in cell culture, while the luciferase reporter provides a simple and easy method for quantitating the extent of virus growth and consequently the antiviral activity of test compounds. The NLRepRLuc/SacII virus was prepared by transfection of HEK 293T cells using the LipofectAMINE PLUS kit from Invitrogen (Carlsbad, CA) according to the manufacturer, and the virus generated was titered in MT-2 cells, using luciferase enzyme activity as an end point.

Drug Susceptibility and Cytotoxicity Assays. Titrated virus was used to infect MT-2 cells in the presence of serial dilutions of ALLINI compounds. A 10 mM stock compound in 100% DMSO was used to make the serial dilutions. Final DMSO concentration in each well was 1%. After 3−4 days of incubation, cells were processed and quantitated for virus growth by the amount of expressed luciferase. Assay medium was RPMI 1640 supplemented with 10% heat inactivated fetal bovine serum (FBS), 100 units/mL penicillin G/100 μg/mL streptomycin, 10 mM HEPES buffer, pH 7.55, and 2 mM L-glutamine. Luciferase was quantitated using Enduren from Promega (Madison, WI). The 50% effective concentration (EC_{50}) was calculated by using the exponential form of the median effect equation where (Fa) = 1/[1+ (ED_{50}/drug conc)^m].[28] Cytotoxicity in MT-2 cells was determined after 4 days incubation using XTT (2,3-bis(2-methoxy-4-nitro-5-sulfophenyl)-2*H*-tetrazolium-5-carboxanilide) to measure cell viability using an established protocol.[29]

Evaluation of in Vitro Metabolism Rates in Liver Microsomes.[30] The metabolic stability (Metstab) assay evaluates cytochrome P450 (CYP)-mediated metabolism of test compounds in vitro using human and rat microsomes after a 10 min incubation. The incubation was automated on a Biomek FX automation workstation (Beckman Coulter, Fullerton, CA, USA). Each compound was incubated in duplicate in the respective species at a concentration of 0.5 μM. Compounds were received as 3.5 mM solutions in DMSO and were diluted with CH_3CN to 50 μM before being added to the prewarmed (37 °C) microsomal suspension (1 mg/mL) prepared in 100 mM sodium phosphate, pH 7.4, and 6.6 mM $MgCl_2$. The reaction was initiated by adding 17 μL of prewarmed 5 mM NADPH in 100 mM sodium phosphate, pH 7.4, into 153 μL of reaction mix. The concentration of DMSO in the incubation mixture was 0.014%. Reaction components were mixed well, and 75 μL was transferred into 150 μL of quench solution at 0 min time point (t0) and again at the 10 min incubation time point (t10). Quenched mixtures were centrifuged at 1500 rpm in an Allegra X-12 centrifuge (Beckman Coulter) for 15 min, and 90 μL of the supernatant was then transferred to a separate 96-well plate for analysis. Metabolism rate was determined based on the parent compound disappearance over time, as measured by LC−MS/MS.

https://dx.doi.org/10.1021/acs.jmedchem.9b01681
J. Med. Chem. XXXX, XXX, XXX−XXX

PAMPA Evaluation. PAMPA assay was conducted in a sandwich setup, consisting of the donor and acceptor chambers separated by an artificial lipid membrane. Test compound (100 μM) was diluted with donor buffer at pH 7.4 and placed in the donor side and allowed to permeate to the acceptor side through the artificial membrane over a 4 h incubation. After incubation the "sandwich" plate was separated. The donor and acceptor solutions, along with the t0 solution, were then measured with a UV plate reader, and the permeability value was calculated by pION software.

In Vivo Rat PK Studies. All animal studies were performed under the approval of the Bristol-Myers Squibb Animal Care and Use Committee and in accordance with the Association for Assessment and Accreditation of Laboratory Animal Care. The pharmacokinetic profiles of **27**, **28**, and **29** were determined in male Sprague-Dawley rats. Animals were dosed iv by cannula implanted in an acceptable vein with an infusion period of 10 min for rats. Animals were dosed orally by gavage following an overnight fast. The vehicle for both iv and po studies was 10% dimethylacetamide (DMAC)/90% PEG400. Blood was collected via a venous port and centrifuged to obtain plasma. Samples were treated with CH_3CN containing an internal standard, centrifuged, and analyzed by LC−MS/MS. Pharmacokinetic parameters were obtained by noncompartmental analysis of plasma concentration versus time data (KINETICA software).

■ ASSOCIATED CONTENT

Supporting Information

The Supporting Information is available free of charge at https://pubs.acs.org/doi/10.1021/acs.jmedchem.9b01681.

Crystallography data for compounds (*S*,*S* and *R*,*R*)-**14** and (*S*,*R* and *R*,*S*)-**15**; crystallization, data collection, and structure refinement results for the HIV-1 integrase CCD:(*S*,*S*)-**14** complex (PDF)

Molecular formula strings and some data (XLSX)

Accession Codes

The coordinates of the HIV-1 integrase CCD:(*S*,*S*)-**14** complex have been deposited in the PDB under PDB code 6UM8. Single crystal structures for (*S*,*S* and *R*,*R*)-**14** and (*S*,*R* and *R*,*S*)-**15** have been deposited in the CCDC database under CCDC deposition numbers 1862636 and 1862637, respectively.

■ AUTHOR INFORMATION

Corresponding Authors

Guo Li − *Department of Early Discovery Chemistry, Bristol-Myers Squibb Research and Development, Wallingford, Connecticut 06492, United States*; Email: guo.li@bms.com

Annapurna Pendri − *Department of Early Discovery Chemistry, Bristol-Myers Squibb Research and Development, Wallingford, Connecticut 06492, United States*; orcid.org/0000-0002-6070-5171; Email: annapurna.pendri@bms.com

Authors

Nicholas A. Meanwell − *Department of Chemistry, Bristol-Myers Squibb Research and Development, Wallingford, Connecticut 06492, United States*; orcid.org/0000-0002-8857-1515

Mark R. Krystal − *Department of Virology Discovery Biology, Bristol-Myers Squibb Research and Development, Wallingford, Connecticut 06492, United States*

David R. Langley − *Department of Computer-Aided Drug Design & Molecular Analytics, Bristol-Myers Squibb Research and Development, Princeton, New Jersey 08543-4000, United States*

B. Narasimhulu Naidu − *Department of Chemistry, Bristol-Myers Squibb Research and Development, Wallingford, Connecticut 06492, United States*

Prasanna Sivaprakasam − *Department of Computer-Aided Drug Design & Molecular Analytics, Bristol-Myers Squibb Research and Development, Princeton, New Jersey 08543-4000, United States*

Hal Lewis − *Department of Molecular Structure and Design, Bristol-Myers Squibb Research and Development, Princeton, New Jersey 08543-4000, United States*

Kevin Kish − *Department of Molecular Structure and Design, Bristol-Myers Squibb Research and Development, Princeton, New Jersey 08543-4000, United States*

Javed A. Khan − *Department of Molecular Structure and Design, Bristol-Myers Squibb Research and Development, Princeton, New Jersey 08543-4000, United States*

Alicia Ng − *Department of Materials Science, Bristol-Myers Squibb Research and Development, Wallingford, Connecticut 06492, United States*

George L. Trainor − *Department of Chemistry, Bristol-Myers Squibb Research and Development, Princeton, New Jersey 08543-4000, United States*

Christopher Cianci − *Department of Virology Discovery Biology, Bristol-Myers Squibb Research and Development, Wallingford, Connecticut 06492, United States*

Ira B. Dicker − *Department of Virology Discovery Biology, Bristol-Myers Squibb Research and Development, Wallingford, Connecticut 06492, United States*

Michael A. Walker − *Department of Chemistry, Bristol-Myers Squibb Research and Development, Wallingford, Connecticut 06492, United States*

Zeyu Lin − *Department of Virology Discovery Biology, Bristol-Myers Squibb Research and Development, Wallingford, Connecticut 06492, United States*

Tricia Protack − *Department of Virology Discovery Biology, Bristol-Myers Squibb Research and Development, Wallingford, Connecticut 06492, United States*

Linda Discotto − *Department of Virology Discovery Biology, Bristol-Myers Squibb Research and Development, Wallingford, Connecticut 06492, United States*

Susan Jenkins − *Department of Pharmaceutical Candidate Optimization, Bristol-Myers Squibb Research and Development, Wallingford, Connecticut 06492, United States*

Samuel W. Gerritz − *Department of Early Discovery Chemistry, Bristol-Myers Squibb Research and Development, Wallingford, Connecticut 06492, United States*

Complete contact information is available at: https://pubs.acs.org/10.1021/acs.jmedchem.9b01681

Author Contributions

The manuscript was written through contributions of all authors.

Notes

The authors declare no competing financial interest.
The authors are or were at the time these studies employees and shareholders of Bristol-Myers Squibb.

■ ACKNOWLEDGMENTS

Robert Gentles and Stella Huang are acknowledged for helpful discussions and NMR interpretation. The Bristol-Myers Squibb Department of Discovery Synthesis and BBRC Bangalore, India, are acknowledged for synthetic support. We

thank Wilson Shou, Amy Sarjeant, Xianmei Cai, Bhupinder Sandhu, and Kathy Mosure for help and support.

■ ABBREVIATIONS USED

AIDS, acquired immunodeficiency syndrome; ALLINI, allosteric integrase inhibitor; AUC, area under the curve; CADD, computer-aided drug design; CCD, catalytic core domain; CD4, cluster of differentiation 4; CCR5, C−C chemokine receptor 5; CTD, carboxyl terminal domain; DDQ, 2,3-dichloro-5,6-dicyanobenzoquinone; DIBAL, diisobutylaluminum hydride; DTT, dithiothreitol; EDTA, ethylenediaminetetraacetic acid; FDA, U.S. Food and Drug Administration; gp41, glycoprotein 41; HAART, highly active antiretroviral therapy; HIV-1, human immunodeficiency virus type 1; HLM, human liver microsome; HSA, human serum albumin; IBD, integrase binding domain; IN, integrase; INSTI, integrase strand transfer inhibitor; iv, intravenous; LEDGF, lens epithelium-derived growth factor; PAMPA, parallel artificial membrane permeability assay; PCC, pyridinium chlorochromate; PK, pharmacokinetic; po, per os; RLM, rat liver microsome; SAR, structure−activity relationship; TI, therapeutic index; WT, wild-type

■ REFERENCES

(1) Gubernick, S. I.; Felix, N.; Lee, D.; Xu, J. J.; Hamad, B. The HIV therapy market. *Nat. Rev. Drug Discovery* **2016**, *15*, 451.

(2) Demeulemeester, J.; De Maeyer, M.; Debyser, Z. HIV-1 integrase drug discovery comes of age. *Top. Med. Chem.* **2013**, *15*, 1−52.

(3) Christ, F.; Debyser, Z. The LEDGF/p75 integrase interaction, a novel target for anti-HIV therapy. *Virology* **2013**, *435*, 102−109.

(4) Engelman, A. E. Multifaceted HIV integrase functionalities and therapeutic strategies for their inhibition. *J. Biol. Chem.* **2019**, *294*, 15137−15157.

(5) Poeschla, E. M. Integrase, LEDGF/p75 and HIV replication. *Cell. Mol. Life Sci.* **2008**, *65*, 1403−1424.

(6) Emiliani, S.; Mousnier, A.; Busschots, K.; Maroun, M.; Van Maele, B.; Tempe, D.; Vandekerckhove, L.; Moisant, F.; Ben-Slama, L.; Witvrouw, M.; Christ, F.; Rain, J.-C.; Dargemont, C.; Debyser, Z.; Benarous, R. Integrase mutants defective for interaction with LEDGF/p75 are impaired in chromosome tethering and HIV-1 replication. *J. Biol. Chem.* **2005**, *280*, 25517−25523.

(7) Busschots, K.; Voet, A.; De Maeyer, M.; Rain, J. C.; Emiliani, S.; Benarous, R.; Desender, L.; Debyser, Z.; Christ, F. Identification of the LEDGF/p75 binding site in HIV-1 integrase. *J. Mol. Biol.* **2007**, *365*, 1480−1492.

(8) De Rijck, J.; Vandekerckhove, L.; Gijsbers, R.; Hombrouck, A.; Hendrix, J.; Vercammen, J.; Engelborghs, Y.; Christ, F.; Debyser, Z. Overexpression of the lens epithelium-derived growth factor/p75 integrase binding domain inhibits human immunodeficiency virus replication. *J. Virol.* **2006**, *80*, 11498−11509.

(9) Llano, M.; Saenz, D. T.; Meehan, A.; Wongthida, P.; Peretz, M.; Walker, W. H.; Teo, W.; Poeschla, E. M. An essential role for LEDGF/p75 in HIV integration. *Science* **2006**, *314*, 461−464.

(10) Jurado, K. A.; Wang, H.; Slaughter, A.; Feng, L.; Kessl, J. J.; Koh, Y.; Wang, W.; Ballandras-Colas, A.; Patel, P. A.; Fuchs, J. R.; Kvaratskhelia, M.; Engelman, A. Allosteric integrase inhibitor potency is determined through the inhibition of HIV-1 particle maturation. *Proc. Natl. Acad. Sci. U. S. A.* **2013**, *110*, 8690−8695.

(11) Feng, L.; Sharma, A.; Slaughter, A.; Jena, N.; Koh, Y.; Shkriabai, N.; Larue, R. C.; Patel, P. A.; Mitsuya, H.; Kessl, J. J.; Engelman, A.; Fuchs, J. R.; Kvaratskhelia, M. The A128T resistance mutation reveals aberrant protein multimerization as the primary mechanism of action of allosteric HIV-1integrase inhibitors. *J. Biol. Chem.* **2013**, *288*, 15813−15820.

(12) Desimmie, B. A.; Schrijvers, R.; Demeulemeester, J.; Borrenberghs, D.; Weydert, C.; Thys, W.; Vets, S.; Van Remoortel, B.; Hofkens, J.; De Rijck, J.; Hendrix, J.; Bannert, N.; Gijsbers, R.; Christ, F.; Debyser, Z. LEDGINs inhibit late stage HIV-1 replication by modulating integrase multimerization in the virions. *Retrovirology* **2013**, *10*, 57.

(13) Le Rouzic, E.; Bonnard, D.; Chasset, S.; Bruneau, J. M.; Chevreuil, F.; Le Strat, F.; Nguyen, J.; Beauvoir, R.; Amadori, C.; Brias, J.; Vomscheid, S.; Eiler, S.; Lévy, N.; Delelis, O.; Deprez, E.; Saïb, A.; Zamborlini, A.; Emiliani, S.; Ruff, M.; Ledoussal, B.; Moreau, F.; Benarous, R. Dual inhibition of HIV-1 replication by integrase-LEDGF allosteric inhibitors is predominant at the post-integration stage. *Retrovirology* **2013**, *10*, 144.

(14) Fader, L. D.; Malenfant, E.; Parisien, M.; Carson, R.; Bilodeau, F.; Landry, S.; Pesant, M.; Brochu, C.; Morin, S.; Chabot, C.; Halmos, T.; Bousquet, Y.; Bailey, M. D.; Kawai, S. H.; Coulombe, R.; LaPlante, S.; Jakalian, A.; Bhardwaj, P. K.; Wernic, D.; Schroeder, P.; Amad, M.; Edwards, P.; Garneau, M.; Duan, J.; Cordingley, M.; Bethell, R.; Mason, S. W.; Bos, M.; Bonneau, P.; Poupart, M.-A.; Faucher, A.-M.; Simoneau, B.; Fenwick, C.; Yoakim, C.; Tsantrizos, Y. Discovery of BI 224436, a noncatalytic site integrase inhibitor (NCINI) of HIV-1. *ACS Med. Chem. Lett.* **2014**, *5*, 422−427.

(15) Tsantrizos, Y. S.; Bailey, M. D.; Bilodeau, F.; Carson, R. J.; Coulombe, R.; Fader, L.; Halmos, T.; Kawai, S.; Landry, S.; Laplante, S.; Morin, S.; Parisien, M.; Poupart, M.-A.; Simoneau, B. Preparation of 2-(*tert*-Butyloxy)-2-(2-methylquinolin-3-yl)acetic Acid Derivatives as Inhibitors of Human Immunodeficiency Virus Replication. World Patent WO2009/062285A1, 2009.

(16) Fader, L. D.; Carson, R.; Morin, S.; Bilodeau, F.; Chabot, C.; Halmos, T.; Bailey, M. D.; Kawai, S. H.; Coulombe, R.; Laplante, S.; Mekhssian, K.; Jakalian, A.; Garneau, M.; Duan, J.; Mason, S. W.; Simoneau, B.; Fenwick, C.; Tsantrizos, Y.; Yoakim, C. Minimizing the contribution of enterohepatic recirculation to clearance in rat for the NCINI class of inhibitors of HIV. *ACS Med. Chem. Lett.* **2014**, *5*, 711−716.

(17) Fader, L. D.; Bailey, M. D.; Beaulieu, E.; Bilodeau, F.; Bonneau, P.; Bousquet, Y.; Carson, R. J.; Chabot, C.; Coulombe, R.; Duan, J.; Fenwick, C.; Garneau, M.; Halmos, T.; Jakalian, A.; James, C.; Kawai, S. H.; Landry, S.; Laplante, S. R.; Mason, S. W.; Morin, S.; Rioux, N.; Simoneau, B.; Surprenant, S.; Thavonekham, B.; Thibeault, C.; Trinh, T.; Tsantrizos, Y.; Tsoung, J.; Yoakim, C.; Wernic, D. Aligning potency and pharmacokinetic properties for pyridine-based NCINIs. *ACS Med. Chem. Lett.* **2016**, *7*, 797−801.

(18) Tsiang, M.; Jones, G. S.; Niedziela-Majka, A.; Kan, E.; Lansdon, E. B.; Huang, W.; Hung, M.; Samuel, D.; Novikov, N.; Xu, Y.; Mitchell, M.; Guo, H.; Babaoglu, K.; Liu, X.; Geleziunas, R.; Sakowicz, R. New class of HIV-1 integrase (IN) inhibitors with a dual mode of action. *J. Biol. Chem.* **2012**, *287*, 21189−21203.

(19) Gupta, K.; Brady, T.; Dyer, B. M.; Malani, N.; Hwang, Y.; Male, F.; Nolte, R. T.; Wang, L.; Velthuisen, E.; Jeffrey, J.; Van Duyne, G. D.; Bushman, F. D. Allosteric inhibition of human immunodeficiency virus integrase. *J. Biol. Chem.* **2014**, *289*, 20477−20488.

(20) Gupta, K.; Turkki, V.; Sherrill-Mix, S.; Hwang, Y.; Eilers, G.; Taylor, L.; McDanal, C.; Wang, P.; Temelkoff, D.; Nolte, R. T.; Velthuisen, E.; Jeffrey, J.; Van Duyne, G. D.; Bushman, F. D. Structural basis for inhibitor-induced aggregation of HIV integrase. *PLoS Biol.* **2016**, *14*, e1002584.

(21) Cherepanov, P.; Ambrosio, A. L. B.; Rahman, S.; Ellenberger, T.; Engelman, A. Structural basis for the recognition between HIV-1 integrase and transcriptional coactivator p75. *Proc. Natl. Acad. Sci. U. S. A.* **2005**, *102*, 17308−17313.

(22) Davis, F. A.; Vishwakarma, L. C.; Billmers, J. G.; Finn, J. Synthesis of α-hydroxycarbonyl compounds (acyloins): direct oxidation of enolates using 2-sulfonyloxaziridine. *J. Org. Chem.* **1984**, *49*, 3241−3243.

(23) Corey, E. J.; Link, J. O. A general, catalytic, and enantioselective synthesis of α-amino acids. *J. Am. Chem. Soc.* **1992**, *114*, 1906−1908.

https://dx.doi.org/10.1021/acs.jmedchem.9b01681
J. Med. Chem. XXXX, XXX, XXX−XXX

(24) Carlens, G.; Chaltin, P.; Christ, F.; Debyser, Z.; Marchand, A.; Marchand, D.; Voet, A.; De Maeyer, M. Novel Antiviral Compounds. World Patent WO2011/076765A1, 2011.
(25) Peese, K. M.; Allard, C. W.; Connolly, T.; Johnson, B. L.; Li, C.; Patel, M.; Sorensen, M. E.; Walker, M. A.; Meanwell, N. A.; McAuliffe, B.; Minassian, B.; Krystal, M.; Parker, D. D.; Lewis, H. A.; Kish, K.; Zhang, P.; Nolte, R. T.; Simmermacher, J.; Jenkins, S.; Cianci, C.; Naidu, B. N. 5,6,7,8-Tetrahydro-1,6-naphthyridine derivatives as potent HIV-1-integrase-allosteric-site inhibitors. *J. Med. Chem.* **2019**, *62*, 1348−1361.
(26) McCoy, A. J.; Grosse-Kunstleve, R. W.; Adams, P. D.; Winn, M. D.; Storoni, L. C.; Read, R. J. Phaser crystallographic software. *J. Appl. Crystallogr.* **2007**, *40*, 658−674.
(27) Emsley, P.; Lohkamp, B.; Scott, W. G.; Cowtan, K. Features and development of Coot. *Acta Crystallogr., Sect. D: Biol. Crystallogr.* **2010**, *66*, 486−501.
(28) Johnson, V. A.; Byington, R. T. Infectivity Assay. In *Techniques in HIV Research*; Stockton Press: New York, NY, 1990.
(29) Weislow, O. S.; Kiser, R.; Fine, D. L.; Bader, J.; Shoemaker, R. H.; Boyd, M. R. New soluble-formazan assay for HIV-1 cytopathic effects: application to high-flux screening of synthetic and natural products for AIDS-antiviral activity. *J. Natl. Cancer Inst.* **1989**, *81*, 577−586.
(30) Kieltyka, K.; Zhang, J.; Li, S.; Vath, M.; Baglieri, C.; Ferraro, C.; Zvyaga, T. A.; Drexler, D. M.; Weller, H. N.; Shou, W. Z. A high-throughput bioanalytical platform using automated infusion for tandem mass spectrometric method optimization and its application in a metabolic stability screen. *Rapid Commun. Mass Spectrom.* **2009**, *23*, 1579−1597.

https://dx.doi.org/10.1021/acs.jmedchem.9b01681
J. Med. Chem. XXXX, XXX, XXX−XXX